# Partial Discharge Classification Using Acoustic Signals and Artificial Neural Networks and its Application in detection of Defects in Ceramic Insulators.

By

Satish Kumar Polisetty

A thesis
presented to the University of Waterloo
in fulfillment of the
thesis requirement for the degree of
Masters of Applied Science

In
Electrical and Computer Engineering

Waterloo, Ontario, Canada, 2019

# Author's Declaration

I hereby declare that I am the sole author of this thesis. This is a true copy of the thesis, including any required final revisions accepted by my examiners.

I understand that my thesis may be made electronically available to the public.

# Abstract

Online condition monitoring of critical assets constitutes one method whereby the electrical insulation industry can help safeguard grids through the avoidance of system outages due to insulation failure. This thesis introduces a novel approach for monitoring the condition of outdoor ceramic insulators based on partial discharge (PD) measurements. The presence of physical defects such as punctures, broken porcelain, and cracks will ultimately lead to the initiation of PD activity in outdoor ceramic insulators. In addition to defects, surface discharges such as that caused by corona and dry band arcing are also very common, particularly in wet and polluted outdoor insulators. Such a discharge activity that originates in these kinds of conditions can cause flashover or insulator failure, resulting in power outages. Measuring early-stage discharge activity is thus very important as a means of avoiding catastrophic situations in power networks.

The work presented in this thesis involved initial tests conducted to distinguish between different types of controlled discharges generated in the laboratory. The next step was the implementation of an artificial neural network (ANN) for classifying the type of discharge based on selected features extracted from the measured acoustic signals. First, relatively high-frequency acoustic signals are transformed into low-frequency signals using an envelope detection algorithm imbedded in the commercial acoustic sensor. A fast Fourier transform (FFT) is then applied to each low-frequency signal, and finally, 60 Hz, 120 Hz, and 180 Hz are used as input feature vectors for the developed ANN.

This initial research was then extended to include testing of the proposed diagnostic tool on a practical insulation system, and outdoor ceramic insulators were selected for this purpose. Three types of defects were tested under laboratory conditions: a cracked ceramic insulator, a healthy insulator contaminated by wetting with salt water, and a corona generated from a thin wire wound to the ceramic insulator. Both a single disc, and three discs connected in an insulator string were tested with respect to these defects. For both controlled samples and full insulators, a recognition rate of more than 85 % was achieved.

# Acknowledgements

This work was carried out during the years 2016-2018 at the High Voltage Engineering Laboratory (HVEL) in University of Waterloo.

I owe my deepest gratitude to my supervisor Professor and Director, Dr. Shesha Jayaram for providing me the opportunity to take part in the research work. I am so grateful for her continuous encouragement, enthusiasm and guidance, without her support this study would hardly have been completed. I also express my warmest gratitude to my other supervisor, Dr. Ayman El-Hag, who suggested this topic to me and encourage me to work in this arear of research. He stood behind me and uplifted me from my low strength areas. His optimistic approach and constant guidance into the world of condition monitoring of line insulators and analysis with machine learning tools have been essential during this work.

I want to express my gratitude to Mr. Mohana Krishnan, HVEL Manager, who helped me to get familiar with the available high voltage technology in the laboratory. He helped me a lot to make possible some of the complex experimental setups for this research work and also shared a deep insight about the condition monitoring aspects.

My thanks goes to Dr. John Long and Dr. Sahar Pirooz Azad who honored me by being on the committee of my thesis examination.

Many thanks are due to my friends at HVEL and colleagues Alireza Naeini, Dr. Khadija Khanum, Faizal, Arathi valal and Marcelo Fernando Cunha for the wonderful time we spent together. Their dedication towards research always inspires me. My special thanks to my great friends Anurag Anand Devadiga and Mahin Parvez for supporting me during both good and bad times.

I would like to acknowledge the financial support from Natural Science and Engineering Research Council of Canada (NSERC) and the faculty Graduate studies, university of Waterloo.

Last but not least, my special thanks to Ms. Barbara Trotter for proof reading my thesis.

# Dedication

*To my Parents, who gifted me this life and shared the deepest love in the world.*

*To my brothers, who constantly believe and respect my every decision in life.*

# Table of Contents

# List of Tables

# List of Figures

# Chapter 1

# Introduction

"Partial discharge (PD) may be defined as a localized electrical discharge that only partially bridges the insulation between conductors" [1]. When an electrical equipment is energized, the presence of defects like cavities, impurities and protrusions outside the insulator can result in the creation of inhomogeneous fields, which eventually initiate PD. Partial discharge includes a wide group of discharge phenomena: internal discharges occur in voids or cavities within solid and liquid dielectrics, surface discharges can be witnessed at the boundaries of different insulation materials, and corona discharges appear in gaseous dielectrics. PD that can be observed at the commissioning of high-voltage electrical equipment is generated because of poor design, workmanship, or improper installation. PD can also be initiated due to the aging of an insulation system. Early-stage detection of PD in the insulation system of any power equipment reduces the risk of total breakdown.

The recent rapid growth in technology has accentuated the necessity for a reliable supply of electric energy. The insulation system plays an important role in transferring the energy produced from generating stations to load points. When both the transmission and distribution of power through overhead lines and underground cables are considered, the transfer of power using overhead lines proves more economical. The central components of an overhead transmission and distribution lines are the tower structure, the line insulators and conductors. Fig. 1.1 shows a detailed view of a typical overhead transmission line.

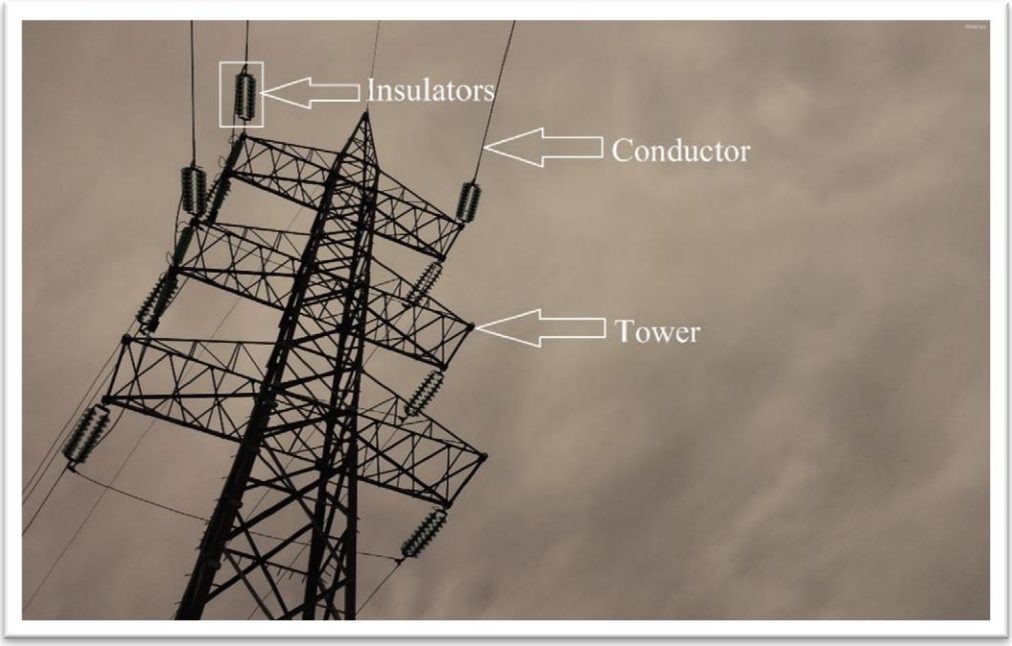


Fig 1.1. Important components of an overhead transmission system [2].

Outdoor insulators are an essential part of a power system because they provide mechanical support for high voltage conductors and also electrically insulate the energized high voltage line from the grounded tower. While fulfilling these functions, outdoor insulators are subjected to electrical, mechanical, and environmental stresses. Electrical stresses are the result of steady-state stresses imposed by operating voltages and transient stresses due to lightning and switching operations [3]. Mechanical stresses include vibrations, tensile and compressive loads under steady-state conditions, and twisting or torsion loads imposed during construction work, and during incidents such as vandalism and vehicle accidents involving poles, which are classified as man-made events [4]. Temperature variations, ultra-violet radiation, moisture, contamination, and wind constitute environmental stresses. All of these stresses vary drastically depending on the design, application, and location of the insulator. Ideally, insulators would be expected to withstand all types of stresses.

Even though outdoor insulators account for only 5% of the total capital cost of overhead line installation, 70% of power outages are associated with deficiencies in outdoor insulator performance, and they represent nearly 50% of line maintenance costs [7]. Outdoor ceramic insulator failure could be due to surface flashover or due to aging. The external surfaces of all insulators eventually become contaminated, and such contamination in the presence of moisture significantly reduces the insulator surface resistance compared to that in

dry conditions. Reduced surface resistance is one of the main negative effects on outdoor insulation performance due to contamination [5]. In humid conditions such as rain and fog, a contaminated insulator surface begins to conduct a leakage current that can cause flashovers which lead to power outages. The capital costs associated with industrial power shutdowns is very high. For example, in the paper industry, a power interruption lasting less than a second can cost up to $50,000 due to lost production [6]. The impact of power outages is even more severe and involves greater capital expense in semiconductor industries.

The degradation of outdoor insulators is another area that creates challenges for North American utilities, with nearly 150 million ceramic outdoor insulators having been in operation for more than 70 years [8]. Undertaking measures for locating the aged line insulators is thus of special interest to utilities. Insulator aging takes a wide range of forms, some of which can be detected visually but others require special testing. The most commonly observed degradation includes punctures, broken discs, and the formation of shaped cracks with varied dimensions. Traditional methods for locating faults in insulators rely on the selection of random samples and their testing in a laboratory [9]. Chapter 2 includes a review and further descriptions of commercial methods currently used in industry and literature about current research conducted with high frequency and acoustic methods. Cost-effective and robust techniques for evaluating faulty insulators under field conditions are always in demand.

This introductory chapter provides a general overview of outdoor insulators. Firstly, the types of outdoor insulators, with a focus on porcelain insulators and their strengths, along with factors that accelerate insulation degradation are discussed. Then the motivation behind the research and the thesis objectives are summarized.

## 1.1 General aspects of outdoor insulators

Especially in the electrical industry, the development of a product that offers advantages over previously established technology always leads to success. With respect to outdoor insulators, this premise is even stronger. The first insulator was put into practical use in 1850, and from then on, the outdoor insulator manufacturing industry has seen numerous improvements. Three main classes of materials are currently used in the manufacture of outdoor insulators: porcelain, glass, and polymers. Porcelain and glass insulators fall under the

heading of ceramic insulators, and polymeric insulators are also called non-ceramic insulators (NCIs) or composite insulators. Each type of outdoor insulator is explained in detail below.

### 1.1.1 Non-ceramic polymeric or composite insulators

Polymeric insulators, also known as composite or non-ceramic insulators, presently dominate the insulator market and are being embraced by utilities. Polymeric insulators represent 60 % to 70% of newly installed insulators [10] and are known for their light weight, resistance to vandalism, superior seismic performance, and flexible design, as well as their hydrophobic nature that enhances their performance under wet and contaminated conditions. A simple polymeric insulator is depicted in Fig. 1.2.

Fig.1.2. A polymeric insulator [11].

Polymeric insulators have three primary components: 1) the core, 2) the housing, and 3) end fittings. Fig. 1.3 shows a cross-section of a polymeric insulator, including construction and material details.

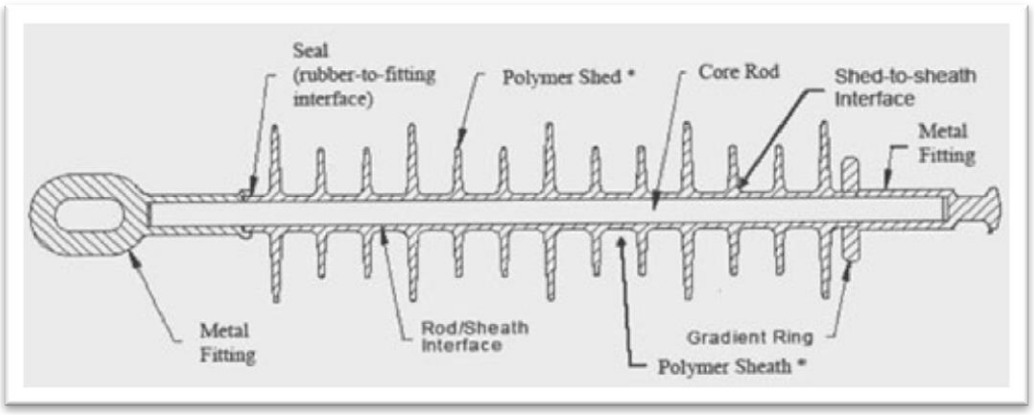


Fig.1.3. Schematic of a typical long rod polymeric insulator [12].

Insulators must be designed to withstand the mechanical loads that are carried by the fibre-reinforced plastic (FRP). The housing is fabricated from rubber polymers, which improves insulator performance by adding hydrophobic properties and by protecting the core from moisture, sunlight, and corona discharge. The end fittings are formed mainly from forged steel that connects the high voltage line to the end of the insulator and the grounded tower. Despite the advantages offered by polymeric insulators, they also have several disadvantages: 1) erosion and tracking can damage these insulators, 2) their surfaces can be subject to chemical changes due to dry band arcing and weathering, 3) detecting faults is challenging, 4) determining their life expectancy and long-term reliability are difficult.

## 1.1.2 Ceramic insulators

Ceramic insulators have been in use for more than one hundred years, during which numerous shell profiles and attachment hardware designs have been developed. The primary constituents of ceramic insulators are their dielectric material, which is the fired ceramic shell, and their hardware, which consists of an iron cap and a pin. The primary objective of adding metallic hardware to the insulator shell is to enable the materials to endure the mechanical loading of the conductors. Fig. 1.4 is a schematic diagram of a single disc of a ceramic insulator. Based on the applied voltage and the pollution levels, a specific number of ceramic discs are connected in series to form a string insulator. While ceramic insulators include both porcelain and glass insulators, the work conducted for this thesis was concentrated on porcelain insulators only.

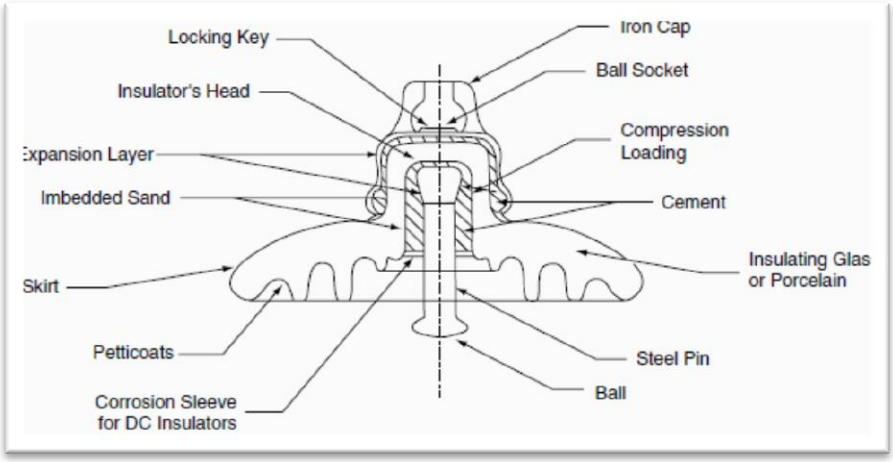


Fig.1.4. Schematic of a typical cap and pin ceramic insulator [13].

## 1.2 Electrical performance of porcelain insulators

Both the internal integrity and the external properties of porcelain insulators determine their overall performance. For example, a void or puncture in the insulator reduces its dielectric strength. Since the dielectric constant of porcelain is greater than that of air, the electric field in a void is intensified and creates a discharge, which can eventually damage the insulator. In addition, the surface properties affect the conductivity status of the insulator shell. Under polluted and humid conditions, the surface conductivity of the insulator increases and can initiate discharge arcs, called dry band arcs, which can lead to insulator flashover.

## 1.3 Porcelain insulator failure

As discussed above, insulators must withstand both the normal system voltage under a variety of weather conditions and the transients that occur due to lightning and switching operations. Porcelain insulators have been used in networks for a long time, and many of them might already have been in service beyond their expected life span. Although some of these older insulators are still functioning satisfactorily, many show serious defects such as cracks, punctures, rusted metal fittings, and broken porcelain. The following sections highlight a number of porcelain insulator defects.

### 1.3.1 Cement growth

Cement growth can create radial cracks inside insulators, as depicted in Fig. 1.5. Cement can absorb moisture during wet conditions, thus escalating the expansion process. Cherney, et al. [14], studied the influence of water expansion on insulator failure. The researchers also carried out autoclave tests on insulators constructed using two distinct types of cement. Their results revealed that the critical length for insulator failure is nearly 0.12 % of the expansion limit for a suspension insulator.

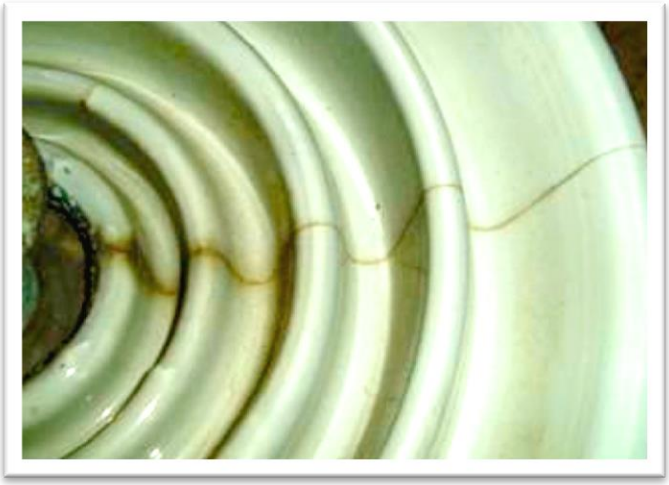

Fig.1.5. A radial crack due to cement growth [15].

### 1.3.2 Hardware corrosion

Corona discharge can occur as a result of inappropriate electric stress grading at the cap of the insulator near the line end of a string of insulators. The metallic cap subsequently becomes exposed to corrosion as the discharge slowly degrades the protective galvanizing layer. Leakage current may also flow on the surface of the insulator during contamination and wet atmospheric conditions, which create a salt solution on the surface. Pin corrosion produced by electrolytic action can weaken the mechanical and cross-sectional strength of the pin. Damage of this sort can lead to an event as serious as conductor dropping. Fig. 1.6 is an example of hardware exhibiting a very high degree of corrosion.

Fig 1.6. Corroded pins in suspension-type porcelain and glass insulators [16].

### 1.3.3 Insulator contamination

Under humid and moist conditions, surface contamination can cause flashover, which leads to system outages. Dust, rubber particles, sand, industrial pollution, and salt from the sea are some of the primary sources of insulator surface contamination. The deposition of contaminating particles is dependent on a number of factors, such as the speed and direction of the wind, the insulator type, and the orientation of the transmission line. Although, rain and heavy winds can wash away dust accumulated on insulators' surface; the dust can still be accumulated on the bottom ribs.

The orientation of the insulator string also influences the amount of contamination. Vertically oriented insulators, also known as an I formation, are prone to greater contamination than are V-shaped and horizontally oriented insulators. During moist conditions, the surface becomes highly conductive and the magnitude of the leakage current increases [17].

Dry band arcing that leads to flashover is the main problem under heavy contamination conditions [18]. Equivalent salt deposit density (ESSD) and non-soluble deposit density (NSSD) are the factors used for quantifying the level of contamination. ESSD is the amount of sodium chloride that, when dissolved, provides the same conductance as that of the natural deposit removed from the surface of the insulator divided by the area of that surface. NSSD is the amount of non-soluble residue removed from a given surface of the insulator divided by the area of that surface.

## 1.4 Condition monitoring of insulators

It is evident that exposure to environmental conditions can accelerate the deterioration of outdoor insulators. The above mentioned defects can thus be further exacerbated, leading to complete insulator failure. Identifying and repairing such defects are therefore critically important. Along with executing health monitoring programs for locating and repairing damaged insulators, utilities are under pressure to reduce their maintenance costs, increase transmission line loading, and improve power quality. Although many inspection techniques are available, most are expensive and time consuming. Even though researchers are working on developing new techniques, many of these new methods are not cost effective or are incompatible with site conditions.

Existing condition monitoring techniques can be classified into two broad categories: offline and online. Offline monitoring techniques take a long time to implement and require the disconnection of energized lines. For these reasons, interest has shifted to online techniques; and some of the important ones are discussed in detail in Chapter 2.

## 1.5 Thesis motivation

The growing demand associated with today's circumstances has brought about a substantial change in the business agendas of utilities worldwide. In contrast to spending a large amount of funds on new assets, the main focus is now shifting towards maximizing the life-time of existing assets. Superior performance and reliability have become important sought-after features of power equipment. Utilizing the complete lifespan of an asset is now a primary goal of utilities, but aging assets represent a greater threat from both financial and performance perspectives because of the increased likelihood of equipment failure [19]. Failed critical assets result in unplanned power shutdowns, causing production losses, environmental issues, and damage to other assets. Taken together, this impact results in millions of dollars in associated costs.

The necessity for utilities to employ economic, innovative, robust and user-safe online techniques for detecting defective porcelain insulators has been constantly growing. In addition to defect detection, a need also exists to discriminate and classify a variety of defects that can occur in porcelain insulators. Researchers are working to develop online condition

monitoring techniques that can change routine periodic maintenance to condition-dependent maintenance, and that can enhance operator's knowledge through information and insight. In an attempt to develop a condition monitoring technique, the focus of the research was on the remote inspection and classification of PD sources using an acoustic technique for data collection and artificial intelligence (AI) for data classification and analysis.

## 1.6 Thesis objectives

The focus of the research conducted in this thesis is to use acoustic sensors for detecting and distinguishing PD that originates from the hardware and a variety of surface conditions. Specific frequency components are extracted from the measured signals and used as input vectors for an intelligent system. An ANN classifier is developed to classify and differentiate the PD sources. Based on this background, the specific objectives of this thesis are as follows:

1) To conduct experiments with a variety of controlled PD sources that represent hardware and surface PD generated under laboratory conditions, and to measure these PD signals using acoustic sensors.

2) To conduct experiments in order to obtain insight into the effect on the acoustic signal amplitude of the captured acoustic signal when the measurement distance and angle are changed from the PD source.

3) To use an ANN pattern recognition tool to conduct a detailed study that will provide an understanding of the potential of the proposed technique to differentiate between different controlled PD sources.

4) To apply the proposed acoustic technique in order to acquire an understanding of the condition of porcelain line insulators. To this end, test samples that represent hardware- and surface-related defects were made in the laboratory. Studies were performed with single and three-disc string insulators connected to the high-voltage source.

5) To investigate the effect of defect types and location in the insulator string on the ANN recognition rate.

## 1.7 Thesis organization

The following is an outline of the thesis:

**Chapter 1** provided a general overview of different outdoor insulators along with their role in the power system networks. Further, the factors accelerating insulation degradation for the porcelain insulators are reviewed; and the objectives of the research are presented.

**Chapter 2** summarizes the online condition monitoring techniques for outdoor line insulators used by power industries, highlighting their advantages and disadvantages, and also providing a review of the literature related to acoustic techniques and high frequency methods.

**Chapter 3** outlines the materials and methods used in this research, describing the controlled PD sources, porcelain insulator samples, experimental setup for PD measurements, signal conditioning, and AI pattern recognition tools.

**Chapter 4** reports the results of the experimental work. The acoustic signals captured in both the time domain and the frequency domain for the controlled PD sources are presented. Using 3-D plots, the patterns formed by the data collected from different controlled PD sources and defective line insulator samples are displayed. Also revealed and discussed are the ANN classifier results to analyze the performance of the classifier using the controlled samples as well as the single disc insulator and the string of insulators. The influence of the distance and angle between the discharge source and the acoustic sensor with respect to the ability of the system to detect a discharge is also explained.

**Chapter 5** presents conclusions based on the research work carried out for the thesis. In addition, future work in the field of the acoustic-based condition monitoring of ceramic insulators are also discussed.

# Chapter 2

# Online Condition Assessment of Outdoor Insulators

## 2.1 Online inspection of outdoor insulators

Methods for detecting defects in ceramic and non-ceramic insulators can be listed as follows:

1) Visual inspection
2) Close contact technique
3) Light-intensified imaging
4) Measurement of the electric field distribution
5) Thermal inspection
6) Electromagnetic emission
7) Acoustic measurements

Each category is briefly described in the following sections.

### 2.1.1 Visual inspection

Visual inspection is an online condition monitoring technique which is considered to be the primary and most commonly used assessment method by many utility companies. A High-powered binoculars or a spotting scope mounted on a stable view point are employed for performing visual inspections. Excessive damage in outdoor insulators, such as broken porcelain, erosion, cracking, splitting, gunshot holes, or punctures as well as hardware damage

due to flashover [20] can be detected through visual inspection. However, internal defects in outdoor insulators cannot be traced using this technique.

## 2.1.2 Close contact technique

One approach most frequently used by utilities for detecting faulty line insulators is close contact method. Used by linemen for inspection, the close contact method is considered low-level technology because the method relies on measuring the resistance of each disc insulator. Two popular instruments developed based on this concept are the buzz meter and the DC insulation resistance-measuring meter developed by Megger®.

The main principle underlying the buzz method is the potential difference across successive bells of an energized insulator string, which are used as a means of detecting a defective insulator. The testing kit consists of a metal prong connected to a hot stick (see Fig 2.1). The prong is placed across each disc of the string individually. If the insulator is healthy, then the potential difference across the electrodes of the disc is enough to create a partial arc that produces a buzzing sound in the small air gap at the tip of the prong. On the other hand, if the disc is defective, then insufficient potential difference exists to produce the arc, and buzzing sound. Small internal defects are often undetected by this measurement.

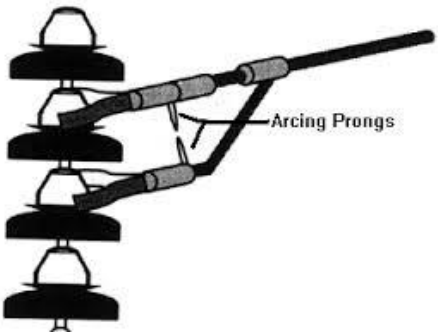


Fig.2.1. Buzz method for finding defects in ceramic insulators [21].

Megger has developed a method to measure the resistance between the cap and pin of each insulator disc under a high-voltage pulse or a DC voltage. The presence of a low resistance indicates a defect in the insulator. Similar to the buzz method, this technique can be used to find surface and very large internal defects. Practical working experience has shown that small internal defects are often not detected.

## 2.1.3 Light-intensified imaging

Light-amplifying equipment can be used for detecting defective outdoor insulators. These devices are able to reveal the presence of surface discharge activity [21], which often marks the beginning of erosion damage or cuts in the housing material. During the night, discharges on the surface of outdoor insulators can frequently be viewed with the naked eye or with the use of a basic night vision camera. However, most of the photons emitted during discharge activity carry energy corresponding to a wavelength of 300 nm to 400 nm (i.e., ultraviolet light), which is beyond the range of visibility for both the human eye and basic light-intensifying devices. To address this problem, ultraviolet (UV) devices have been implemented because they can enhance detection capabilities.

Intensifying the light emitted can enable the early-stage detection of defects [22]. Recent advances have included the development of light-intensifying cameras for detecting coronas in daylight. Commercial corona cameras are used extensively by utilities in the field for detecting levels of pollution on insulators [23]. This type of camera incorporates a video recorder with a UV-intensified image synchronized to a supply voltage. The device utilizes the fact that a corona can occur close to the peak of the supply voltage in order to separate the light emitted by the corona and that emitted by the sun. Using the UV image-intensification feature, two separate images are taken: one with, and one without the corona. After image processing, the final image can be seen by the user [24]. Sample measurements made using a corona camera are shown in Fig. 2.2.

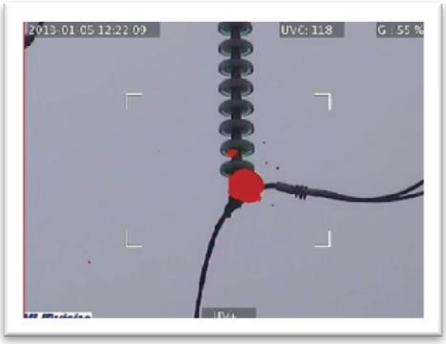


Fig.2.2. Corona discharge detected using UV intensification imaging [25].

### 2.1.4 Measurement of the electric field distribution

The permittivity and conductivity of materials as well as their geometry influence the distribution of the electric field along the insulator surface [26]. The electric field sensor mounted on the top of a rod is brought close to the energized insulators. Sliding the probe along the surface of a string of insulators enables the electric field distribution along the surface to be measured. The presence of a defective insulator in a string causes an abrupt change in the magnitude and direction of the electric field. The data collected through the measurement process is stored in a data logger attached to the probe, and is then transferred to a separate computer, where data are compared with those for a healthy insulator. The electric field measurement technique is applied for both ceramic and composite insulators. This method is used extensively by utilities.

### 2.1.5 Thermal inspection

Thermal inspection methods rely on thermal vision in order to determine the presence of hot and cold areas on insulators as a means of detecting defects. In general, a healthy insulator produces heat near the pin during wet conditions, whereas punctured insulators remain cold. Sensing discrepancies in the surface temperature along the string is very helpful, especially when several defective units are clustered at the live end of the insulator string. This method is used as a pre-test for detecting defects and anomalies registered through infrared (IR) thermography. Close contact or electric field distribution methods are then used for detailed investigation of insulators suspected of failing. A major disadvantage of this method is the sensitivity of the measurements to strong winds, dew, rain, sun radiation, and rapid temperature changes in the surrounding environment [27].

### 2.1.6 Electromagnetic emission

This method is based on the fact that defects in insulators under high voltage produce electromagnetic (EM) signals with different frequency ranges. The commercially available equipment named EXTRACTER monitors the EM noise signals and calculates a quantity referred as “maintenance merit”. When the calculated maintenance merit value exceeds a certain threshold, the device extracts frequencies ranging from the fundamental to the 50th

harmonic (60 Hz to 3 kHz) from the EM noise signal spectrum. The spectrum is updated every second and saved for further analysis and future reference. Although this method has produced promising results in the laboratory, insufficient evidence exists to support the effectiveness, accuracy, and reliability of the technique in the field. Its advantages include enhanced safety, and time and cost savings, which must be weighed against the disadvantage of the requirement for large amounts of data to be collected, processed, and analyzed [28].

Some of the condition monitoring techniques like radio-frequency measurement and ultrahigh frequency measurement techniques are designed to detect EM signals at very-high frequency (VHF), ranging from 30 MHz to 300 MHz, and the ultra-high frequency (UHF) band, from 301 MHz to 3 GHz [29]. Studies indicated that signal-to-noise ratio (SNR) for VHF is lower than that in UHF band due to susceptibility to interference in the lower frequency band. However, long distance measurements, VHF signals experience lower attenuation than those in the UHF band. RF based PD detection techniques have been applied with a reasonable amount of success to gas insulated switchgear (GIS), and transformers, but very little work has been performed with respect to the application in condition monitoring of outdoor porcelain insulators.

### 2.1.7 Acoustic emission

It is well known that defects in insulators produce electrical discharges, which produce sound/acoustic signals. These sound signals can be recorded using sensitive sound sensors. Such acoustic emission (AE) measurement techniques can be used in two ways. The first involves an operator listening to the acoustic signals produced by the object under study through parabolic dish sensors that have very sensitive microphones and high-gain amplifiers. Background noise at the site has been found to interfere with this type of measurement technique [30]. The second method is called the pulse echo method. It enables an examination of the propagation of an acoustic wave through the insulation based on observations of the signal attenuation and changes in velocity and direction associated with the wave. This method is carried out by directing an acoustic signal into the insulation and reading the reflections, which can enable the identification of defects [31].Table 2.1 summarizes the advantages and disadvantages of the methods discussed above.

**Table 2.1: Advantages and Disadvantages of Methods for the Online Monitoring of Line Insulator Condition**

| Technique | Advantages | Disadvantages |
|---|---|---|
| Buzz method (Close contact method) | Very simple in operation | Labour intensive |
| | | Safety of linemen at risk |
| | | Accuracy |
| Megger method (Close contact method) | Very simple in operation | Labour intensive |
| | | Safety of linemen at risk |
| | | Accuracy |
| Light-intensified imaging method | Improved safety compared to close contact method | Expensive equipment |
| | Time saving achieved through inspecting large number of insulators in short amount of time | Inaccurate in sunlight |
| Thermal inspection | Improved safety compared to close contact method | Requires humidity to pick up a defective insulator |
| | Time saving achieved through inspecting large number of insulators in short amount of time | Sensitivity/accuracy |
| | | Expensive equipment |
| Electric field distribution measurement method | Very simple in operation | Labour intensive |
| | More sensitive than buzz and megger methods | Safety of linemen at risk |
| High frequency emission method | Time saving achieved through inspecting large number of insulators in short amount of time | Needs skilled workers |
| | Potential for determining the type of defect | Not well proven for field measurements |
| Acoustic measurement | Safe and simple to operate | Reliability |
| | Time saving achieved through inspecting large number of insulators in short amount of time | Reflections can mislead |
| | | Sensitivity |

A review of the literature related to existing condition monitoring techniques for outdoor insulators reveals ongoing opportunities for further enhancement of the technology. Such developments should take into account the future of prognostic capabilities that can encourage utility authorities obtain sufficient information to make timely and cost-effective decisions. Researchers have reported the potential for high frequency and acoustic methods to

address the condition monitoring of insulation due to their superior immunity to noise and their ease of operation [32], [33].

## 2.2 Robustness of acoustic methods

Earlier, researchers from the HVEL at the University of Waterloo conducted laboratory and field-based studies to distinguish discharges from a string of porcelain insulators with a deliberately introduced cracks, hole through the cap, and a broken disc. The work involves measurement of PD signals using an RF antenna with a bandwidth of 1-2 GHz. Wavelet analysis was conducted to extract features from the measured PD signals, which were fed to an ANN classifier to distinguish between different types of defects. The results showed a recognition rate of 95% [34]. Despite the successful classification using RF technology, there are disadvantages of using RF antenna. Firstly, because of their high-frequency bandwidth, as RF antenna can't measure low-frequency discharges like dry band arcing [32]. Also, the technology suffers from electromagnetic interference (EMI) under field conditions. On the other hand, acoustic sensors can measure all forms of discharges, and since they are measuring mechanical waves, they are immune to electromagnetic interference. Hence, this research has concentrated on using acoustic sensors to detect different forms of defects in ceramic insulators.

High frequency components for AE (16 kHz to 300 kHz) can be used for acquiring information about the condition of the insulation, either through direct listening to the sound produced by the insulation, or capturing the sound echoes. These techniques are known as active and nondestructive testing (NDT) techniques, respectively [35]. The following literature review provides insight into the application of ultrasonic techniques and their benefits with respect to detecting defects in different types of electrical insulation. A cast resin 12 kV bushing failed during a partial discharge test conducted as per IEC 60270. Inspection using NDT ultrasound was able to reveal the presence of a void at the resin conductor interface [36-38]. In a similar situation, several methods failed to detect the defect in a 15 kV resin-impregnated paper insulation bushing. Using an acoustic technique to record the peak-to-peak and root mean square (RMS) values of an acoustic signal along the length of the bushing resulted in determining the fault location.

Acoustic sensors consisting of highly sensitive piezoelectric films with filters, preamplifiers, data acquisition systems, and output devices have been employed for the condition monitoring of high voltage cables. Acoustic techniques for cable insulation diagnosis are not subject to any significant electrical interference, but an acoustic wave travelling along the cable joints and other interfaces may exhibit attenuation. An NDT test performed on 11 kV bundled conductor cable with a central conductor diameter of 6 mm enabled a determination of the location of voids at the interface between the XLPE and the semiconductor sheath. A study conducted as a means of locating the water tree in a similar type of cable proved successful. The repeatable feature in the acoustic signal returned did not appear in the spectra, and the data collected was used for training an ANN. The ANN proved to be 95 % successful in identifying healthy and weak areas in the cable, and demonstrated a success rate of 80 % when tested with different cable specimen. The literature reports that tests conducted using acoustic techniques on cable terminations indicate the possibility of identifying the discharge source and its location [36-38].

A cracked-insulator acoustic probe (CIAP) is a licensed technology developed by Hydro-Québec and used for inspecting live lines. Cracks in a porcelain insulator and any weakening of the metal-porcelain interface due to exposure to harsh weather can be detected using this technology, which has proven successful for locating cracks in high voltage insulators up to 120 kV [39]. The probe comes with two pairs of plastic feelers that consist of a proximity sensor, a small hammer, and a miniature microphone for picking up sound samples. Only three samples taken at different points on the shed are sufficient for tracking the condition of an insulator [39]. Fig. 2.3 displays details of the mounting of the sensor on the insulator.

Fig. 2.3. CIAP feelers probing a 120 kV insulator shed [39].

In other research [40], passive-focused paraboloid acoustic sensors were used to detect sound signals generated from a PD to examine the severity of the pollution on ceramic insulators. Artificial contamination experiments were performed in order to investigate the relationship between AE signals and PD intensity levels. The results revealed a clear distinction with respect to the transition of AE signal waveforms from the initial stage of low contamination levels to the final stage of flashover.

In a similar study [41], an acoustic sensor with a bandwidth of 100 kHz to 1200 kHz was used for recording AE signals from porcelain insulators with cracks, punctures, chipped discs, and voids. These AE signals were compared with signals collected using a high frequency current transformer (HFCT) with a bandwidth of 1 MHz to 100 MHz coupled to the earth connection of the insulator and a conventional PD detection system. The authors reported the distinctive features of the acoustic sensor and the HFCT. They pointed out the attractiveness of AE detection due to its relative immunity to noise, but also noted that its low degree of sensitivity and narrow frequency bandwidth made it inferior to the HFCT method.

Researchers have also employed a commercial acoustic sensor and an ANN to investigate the ability to classify PD signals generated due to dry band arcing, corona signals from sharp electrodes, and mechanical noise signals. An average recognition rate of 93.3 % was achieved [42].

The application of acoustic sensors is not limited to outdoor electrical insulation. The results of studies related to the condition monitoring of transformers and GIS insulation are also very promising [43-46]. Inspired by all of the contributions concentrated on understanding the health condition of insulation using acoustic technology, the research presented in this thesis was conducted with the goal of investigating the possibility of detecting and classifying controlled PD sources and defects in ceramic disc insulators.

## 2.3 Summary

This chapter has provided a summary of available online inspection methods practiced by utilities for the assessment of defective line insulators, including a table list of the advantages and disadvantages of each method. A detailed review of the literature related to acoustic techniques and their successful implementation for the condition monitoring of electrical equipment in power networks has also been presented.

# Chapter 3

# Materials and Methods

Acoustic methods used for detecting electrical discharge are quite popular because of their immunity to electromagnetic noise and their relative ease of application. Controlled PD sources representing a variety of discharge types, such as corona (discharge in air), surface discharge, internal discharge, and wet surface discharge were generated in the laboratory. Based on the test results, and knowledge obtained through the classification of these controlled sources with the use of acoustic sensors, the technique was then applied to detecting defects in outdoor insulators.

This chapter describes the test setup for generating controlled PD sources and also explains different types of PD sources created using porcelain insulators in the experimental work. Details of the experimental setup, data acquisition techniques, and the artificial neural network topology are also provided.

## 3.1 Controlled PD sources

As illustrated in Fig. 3.1, five common types of PD were considered for the multi-class classification analysis: PD from a sharp point, surface discharge from a smooth electrode, surface discharge from a sharp electrode, wet surface discharge from a smooth electrode, and internal discharge from voids.

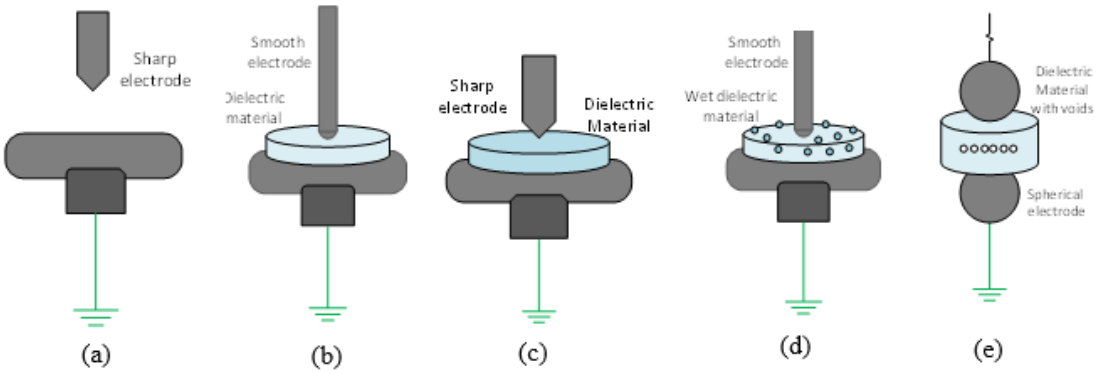


Fig. 3.1. Illustrations of the geometrics of the PD sources used: (a) PD from a sharp electrode; (b) surface discharge from a smooth electrode; (c) surface discharge from a sharp electrode; (d) wet surface discharge from a sharp electrode; (e) internal discharge from a defective dielectric medium.

## 3.2 Porcelain insulator samples

The study involved samples of three PD sources: discharges due to cracks, hardware corona, and wet surface discharge due to surface contamination. Fig. 3.2 shows a ceramic insulator disc with a deliberately introduced crack.

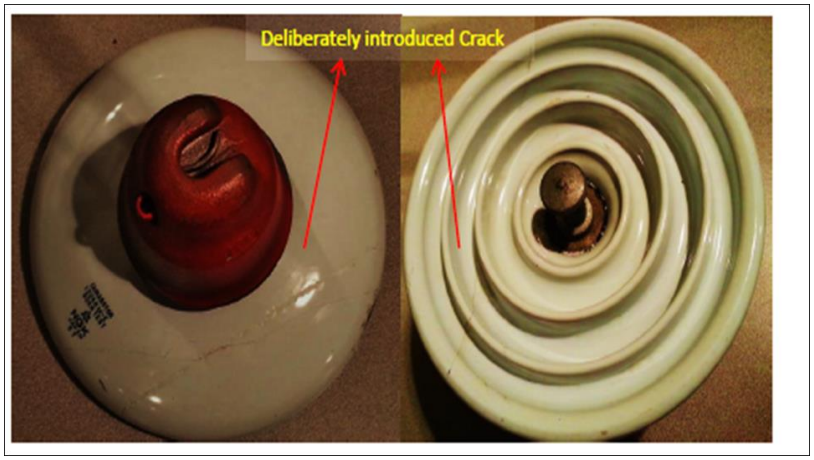


Fig.3.2. Porcelain line insulator with a deliberately introduced crack.

Fig. 3.3 shows a healthy insulator with a thin wire wound around the cap that is used to replicate a hardware corona. This kind of discharge is very common in power systems, but hard to distinguish from other types of severe discharge using the regular online monitoring techniques currently available.


Fig.3.3. Hardware corona generated using a thin wire wound around the cap of a line insulator.

For the third case study, a healthy insulator was sprayed with salt water so that the electrolyte solution acts as a surface pollutant.

## 3.3 Need for ultrasonic measurement

Each PD event produces an ultrasonic emission. Fig. 3.4 indicates the frequency ranges of the different generated acoustic emissions (AEs) including the generated PD AEs. The range considered for measurement using the acoustic sensor in this thesis is from 16 kHz-80 kHz. The range above the 20 kHz is categorized under ultrasonic range of frequencies.

In general, ultrasound provides a very good signal-to-noise ratio, which means that the equipment used for measuring high frequency acoustic emissions can reject high levels of background noise and can focus on a desired range of frequencies.

Audible, low frequency sound waves tend to travel large distances, reflecting from walls, equipment, etc., before diminishing. These reflections add to the background noise in the audible range, whereas, ultrasonic sound cannot travel long distances and is usually softened completely prior to reflection. These high attenuation rates of ultrasonic signals result in low background noise levels, even in the least favorable environments. For example, a typical industrial environment has background audible noise levels up to 100 dB, while only 15 dB of noise is around 40 kHz [47]. For this reason, isolating the desired signal from the

background noise is comparatively easier using ultrasonic sensors than measuring audible acoustic signals.

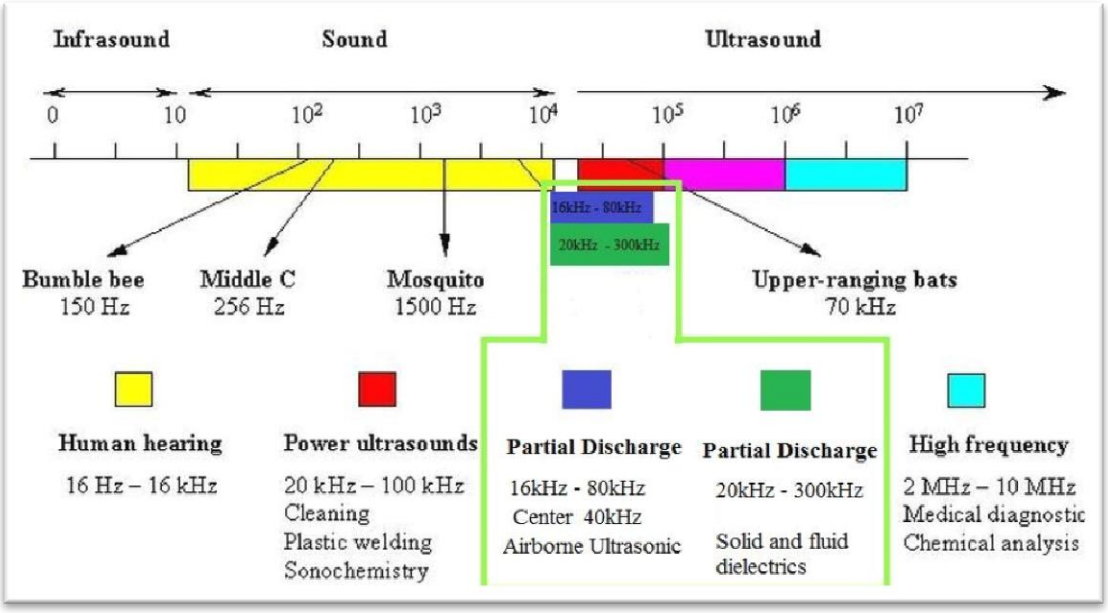


Fig. 3.4. Frequency ranges of different acoustic emissions generated compared to PD acoustic emissions [47].

## 3.4 Airborne ultrasonic sensors

In commercially available airborne ultrasonic sensors, three types of data can be extracted depending on the degree of sophistication, i.e, qualitative, quantitative, and analytical. Qualitative information offers the ability to convert the signals to low frequencies through frequency modulation so that the human ear can hear the ultrasound version. Quantitative information includes details of the intensity (dB) of the measured ultrasonic signal, which are displayed on the instrument screen, and analytical data can be collected from spectral analysis software to enable a review of the recorded sound samples. The sensor used in the research has a combination of qualitative, quantitative and analytical features. In practice, three types of airborne ultrasonic sensors are widely used by utilities: handheld units, parabolic dish concentrators, and extended wand-type sensors. Table 3.1. Illustrates the features of the sensor employed in this research.

**Table 3.1: Features of the MK-720 Acoustic Sensor**

| | |
|---|---|
| Model | MK-720 |
| Detection frequency | Central frequency 40 kHz ( Suitable to measure PD in the range 16 kHz - 80 kHz) |
| Detection directionality | ±8° |
| Dimensions – Net weight | W 174 mm x H 268 mm x D 98 mm – Approx. 370 g |
| Ambient measurement parameters | 0 °C to 40 °C, 10 % to 85 % relative humidity (non-condensing ) |
| Function | Display of discharge component rate; display of converted value in acoustic pressure; alarm based on discharge component rate; measuring point indicated by laser pointer (laser pointer light intensity Class 2 IEC 6825-1) |

## 3.5 Test setup

The schematic of the test setup used for generating and measuring controlled PD from different types of sources is shown in Fig. 3.5. A 150 kV/20 kVA test transformer with a PD level of less than 2 pC. The inception of PD activity was ascertained using a classical PD detector, which employs a coupling capacitor per IEC 60270. For the experimental work, the initial PD inception voltage (PDIV) was measured with the simultaneous use of both a standard PD detector (Hipotronics®, DDX 9101) and the MK-720 acoustic sensor. The PDIV for corona from a sharp electrode was observed at 9.6 kV by the coupling capacitor, and also using the acoustic sensor. This shows that both methods were in good agreement with the inception voltage measurement.

As per the vendor provided datasheet, the acoustic sensor is not sensitive at distances above 2 m from the source of discharge. With consideration of the sensitivity factor and also laboratory safety standards, the sensor was placed 1.6 m from the test setup. Fig. 3.5 shows the arrangement used for testing the porcelain disc insulator.

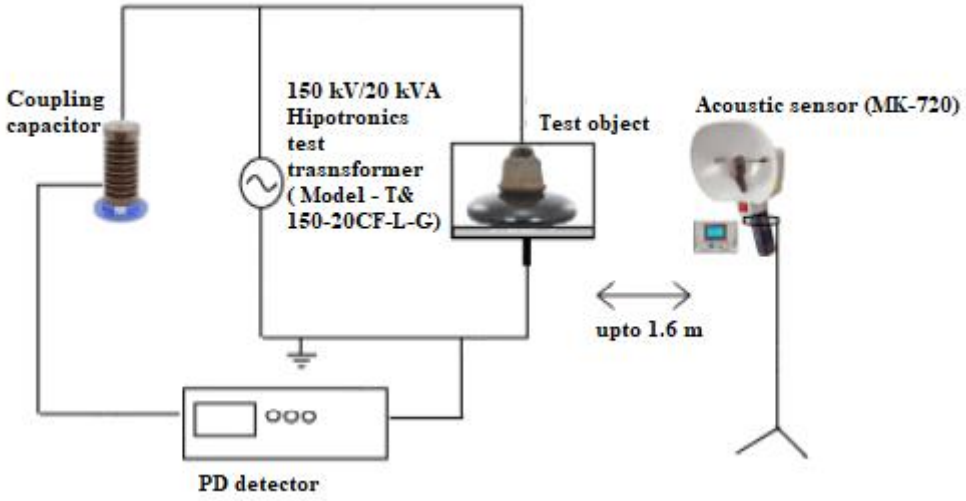


Fig.3.5. Schematic of simultaneous PD measurements using a coupling capacitor and an acoustic sensor.

## 3.6 Signal processing

The output of the acoustic sensor was first run through a high-pass filter (HPF) in order to remove noise, following which, the outer envelope of the filtered signal was detected prior to the final step, which was the application of a fast Fourier transform. The MK-720 acoustic sensor is equipped with the tools necessary for performing these operations on a measured acoustic signal. A typical measured acoustic signal and its FFT from a sharp electrode are shown in Fig. 3.6 and Fig. 3.7, respectively, and the stages involved in the signal processing are identified in Fig. 3.8.

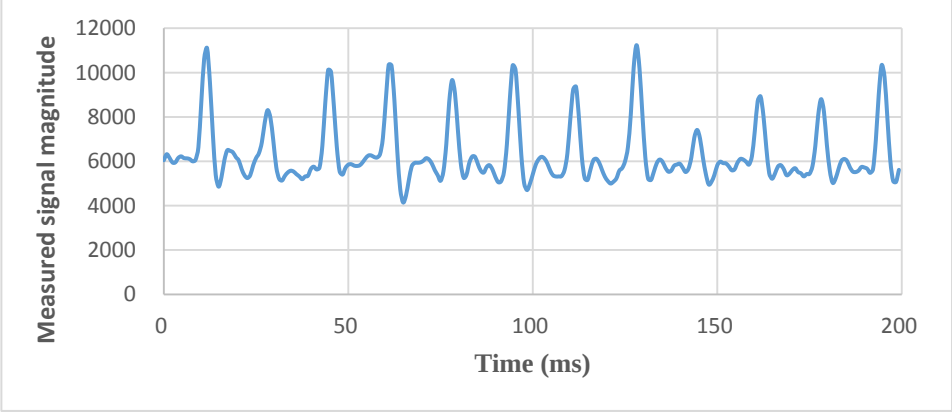


Fig.3.6. Example of acoustic signal measured using the MK-720 from a sharp electrode.

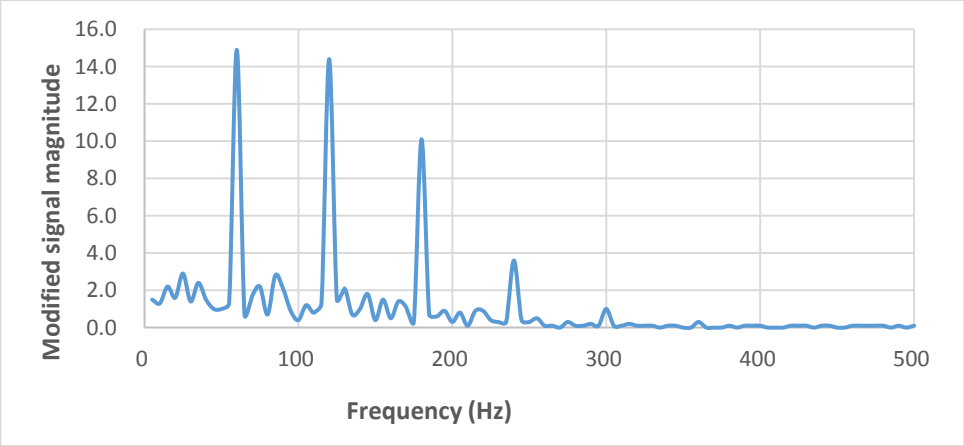


Fig.3.7. Typical FFT of a PD acoustic signal acquired using the MK-720 from a sharp electrode.

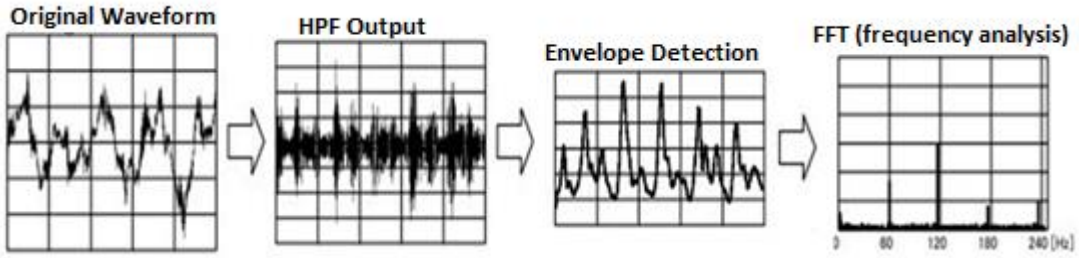


Fig.3.8. Envelope detection and FFT operations for converting the measured acoustic signals from time domain to frequency domain [46].

The intensity of the ultrasound emitted from a PD source varies periodically with the alternating voltage. The acoustic sensor uses the amplitude modulation technique where carrier wave with particular frequency is changed according to the intensity of the audio signal. Here, the sensor has inbuilt technology to use carrier waveform frequency same as supply voltage frequency [48], which means that the amplitude spikes of the processed acoustic signal dominate at the fundamental frequency of the supply voltage and its integral multiples. Details of the signal strength for 60 Hz, 120 Hz, and 180 Hz frequency components were used for analysis. The analysis process and the tools used for the classification of the discharges are presented in Chapter 4.

## 3.7 Artificial neural network

Machine learning (ML) is an element of AI and is currently widely used in many applications. It refers to the science of using signal processing, mathematical, and statistical tools for making interpretations based on perceptual data. Reliable and accurate ML is very

useful and some of the successful implementations can been seen in fingerprint identification, DNA sequence identification, automated speech recognition, etc. ML systems differ, but all involve three essential stages: 1) data acquisition and preprocessing 2) feature extraction and 3) decision making.

In data acquisition and preprocessing, the data are collected from the source and then preprocessed to filter out noise or outliers. Users must define the relevant features for identifying different patterns. In the final stage, the ML algorithm performs the desired operation of either classification or regression.

In the work presented here, the PD signals collected using the acoustic sensor described earlier are passed through multiple signal processing operations and the three frequency components are recorded, i.e., 60 Hz, 120 Hz and 180 Hz. The dominant frequency components can then be used as input feature vectors to train the selected classifier, which for this study, is an artificial neural network. These models are computing systems that consist of a very large number of processors that have been interconnected so that they can handle huge amounts of data. ANN models are typically self-adaptable with respect to learning and resolving complex problems based on available training and knowledge, thus giving rise to their name. ANNs are designed to work like a biological brain, with the interconnected processors functioning in a manner similar to that of neurons. The interconnections enable data to be transferred between neurons. The learning process determines the weights applied to the connections, which in turn, indicate the importance of the contribution of the preceding neurons. Fig. 3.9 and Fig. 3.10 illustrate the structures of the ANNs used for developing the classifier for this research.

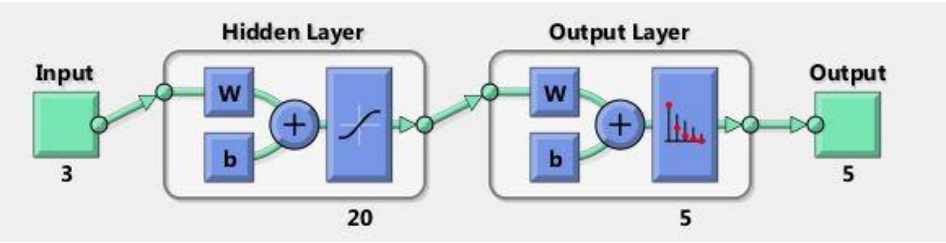


Fig.3.9. Structure of the ANN implemented in the analysis conducted for distinguishing types of PD from controlled PD sources: three input feature vectors, 20 hidden neurons, and five output classes.

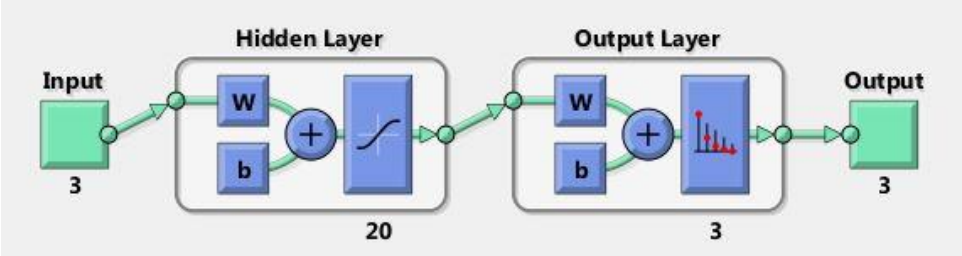


Fig.3.10. Structure of the ANN implemented in the analysis conducted for distinguishing types of PD from the porcelain insulators used in the case study: three input feature vectors, 20 hidden neurons, and three output classes.

Each element in the structures consists of input, hidden and output layers: The input layer communicates with the external environment to manage all of the input and present it to the neural networks. The input feature vectors are composed of the magnitudes of 60 Hz, 120 Hz, and 180 Hz frequency components of the received signal.

The hidden layer lies between the input and output layers and consists of activation functions. The role of the hidden layer is to process the input obtained from the previous layer. The number of hidden layers plays a crucial role in determining the performance of the classifier. In this research, only one hidden layer was used with variable number of hidden neurons. Fig.3.11 displays the average recognition rate plotted against the number of hidden neurons. The graph reveals that the additional hidden neurons gradually increase the average recognition rate until it reaches a saturation level.

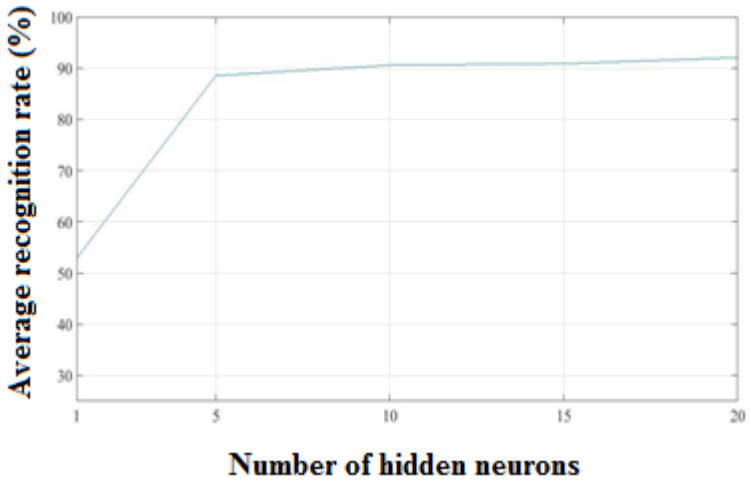


Fig.3.11. Graph showing the variation in test efficiency with increased numbers of hidden neuron.

The output layers act as information interfaces from the system to the output classes. In the work conducted for this thesis, controlled PD sources are represented as class-I (wet surface discharge from a smooth electrode), class-II (designating surface discharge from a smooth electrode), class-III (internal discharge from defective dielectric material), class-IV (surface discharge from a sharp electrode), and class-V (corona). For the study of the porcelain line insulators, class-I represents corona, class-II designates discharge from a cracked line insulator, and class-III refers to discharge from a contaminated surface.

## 3.8 Summary

This chapter has outlined the materials and methods employed for the research. Particulars have been provided for the five controlled PD source setups used for the initial studies and for the different defective samples of porcelain insulators on which the new technique was applied. Other components explained in detail include a schematic of the test setup with the specifications for the acoustic sensor employed in the study, and the signal processing methods used for extracting features for further analysis.

# Chapter 4

# Results and Discussion

As described in Chapter 3, the extracted features (low-frequency components) were used for training and testing the developed classifier. Classification performance results for controlled PD sources, single-disc insulators, and string insulators were represented visually using 3D plots and then assessed using the ANN classifier. The effect on the efficiency of the proposed technique with respect to a number of factors, such as variations in the linear and angular distance of the acoustic sensor is also discussed in this chapter.

## 4.1 Characteristics of the controlled PD signatures

As previously discussed, both acoustic signal envelopes and their FFTs were captured for different types of controlled PD. Fig. 4.1 shows examples of signal results captured from a sharp electrode (corona), and wet surface discharge from a smooth electrode.

It is apparent that each discharge type has a signature distinguishable from those noted with other types of discharges. For example, the amplitude and repetition rate of the spikes are relatively high for the discharge from sharp electrodes compared to those from a smooth electrode. With respect to the frequency content of the measured envelope, it can also be observed that the corona discharge has a more consistent pattern than the wet surface discharge. Differences in the acoustic signal signatures are due to the nature of the streamers

formed as a result of the ionization of the air surrounding the electrode and the dielectric medium.

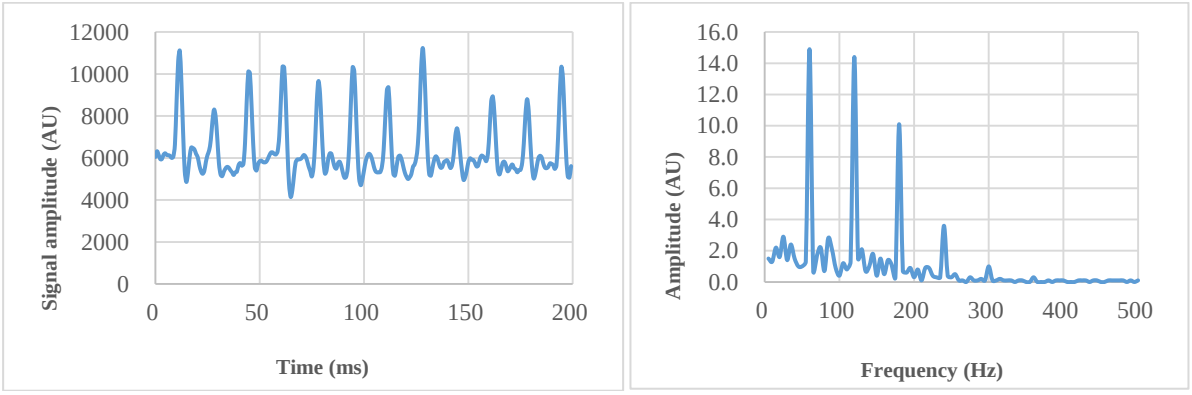


(a)

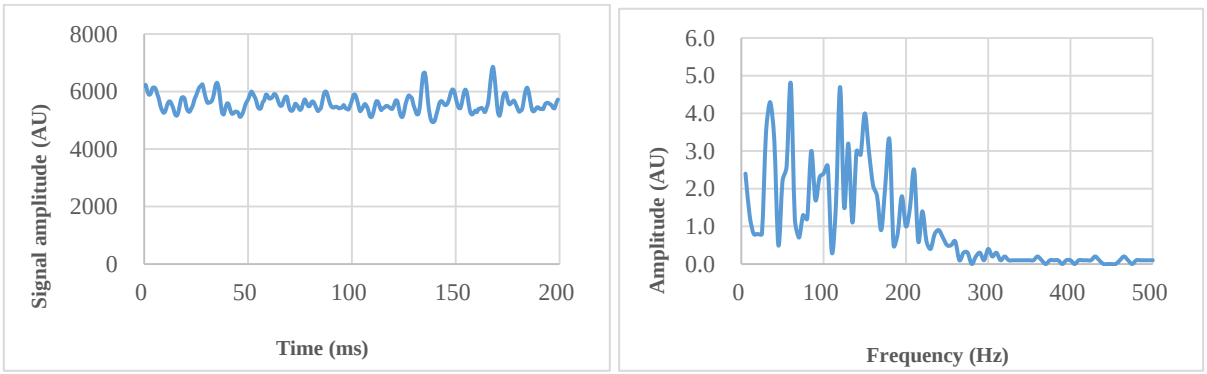


(b)

Fig.4.1. Signal envelopes of the acoustic signals and their FFTs measured from (a) discharge produced by a sharp electrode, and (b) wet surface discharge produced by a smooth electrode.

## 4.2 Influence of distance on acoustic PD signal measurements

To examine the influence of distance on the measurements obtained from the acoustic sensor for two different discharges (i.e., the corona discharge and the surface discharge), measurements were made using a sharp electrode at 150 cm, 200 cm, 250 cm, and 300 cm from the test sample. Regardless of the type of discharge, the acoustic sensor was able to detect PD signals even at a distance of 300 cm. These results demonstrate that the technique can be used at a safe distance for overhead distribution line inspection.

The results related to the attenuation rate of the measured acoustic signal frequency components with discharges from a sharp electrode in air (corona) and from a dielectric medium (surface discharge) are shown in Fig. 4.2 and Fig. 4.3, respectively.

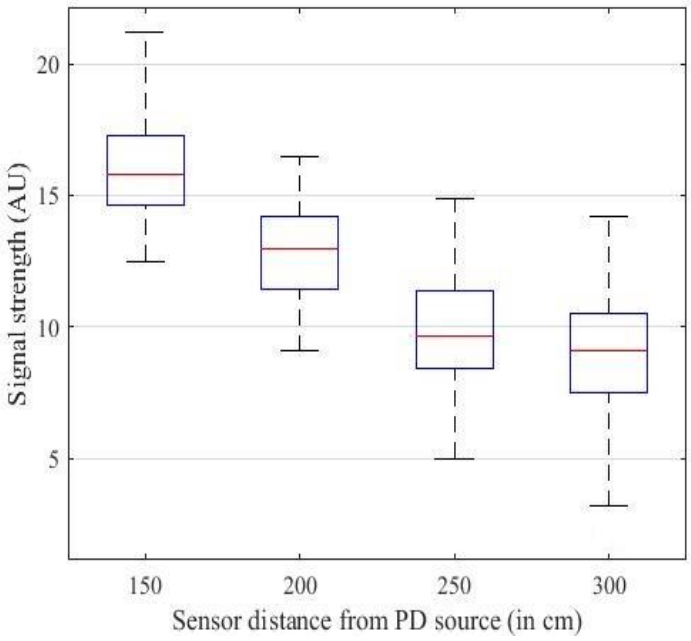


Fig.4.2. Attenuation of the signal strength with distance for a 60 Hz component with corona discharge.

The results reveal that a decreasing trend in the amplitude of the acoustic signal strength can be observed in the corona with the 60 Hz component. A similar trend with the signal strength was noted with 120 Hz and 180 Hz components.

On the other hand, for a surface discharge, only the 120 Hz component exhibits a decreasing trend similar to that for a corona. No consistent trend can be observed for either the 60 Hz or the 180 Hz components. However, for both types of discharge, the total signal strength decreases with distance.

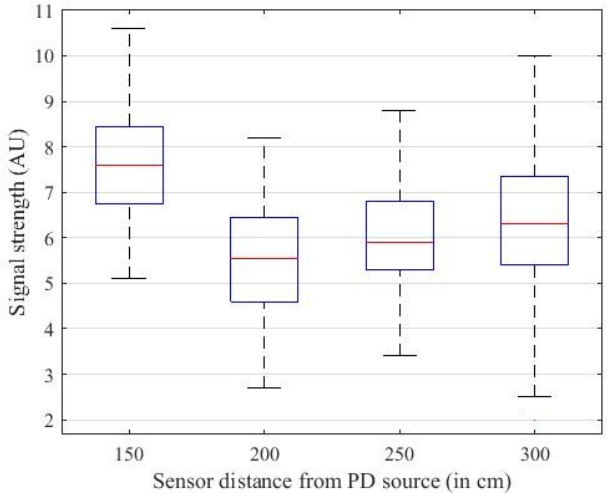


(a)

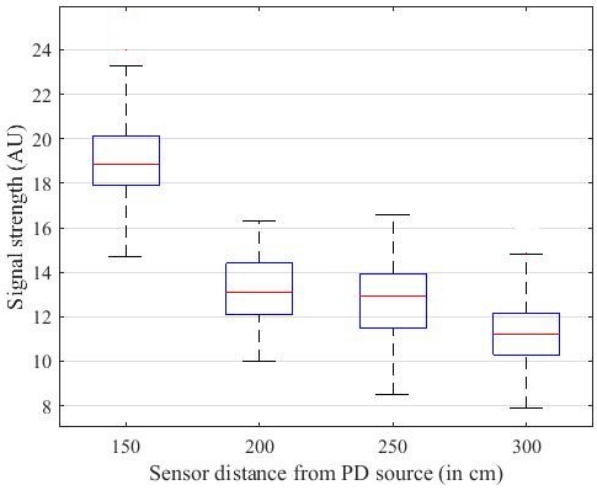


(b)

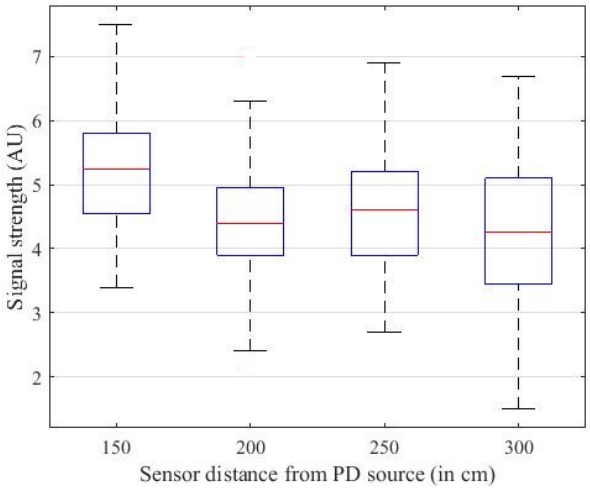


(c)

Fig.4.3. Attenuation of the signal strength with distance with a surface discharge for (a) a 60 Hz component, (b) a 120 Hz component, and (c) a 180 Hz component.

## 4.3 Influence of the angle of measurement on the acoustic PD signal

Fig.4.4 shows the test setup arrangement for studying the effect of measuring angle on acoustic signal measurement. The attenuation of the signal strength as a result of changes in the angle of measurement from the corona was investigated. The results are shown in Fig.4.5.

The results reveal that as the angle of deviation from the PD source increases, the 60 Hz component is subject to minimum attenuation. Similar behaviour was observed for the 120 Hz and 180 Hz components.

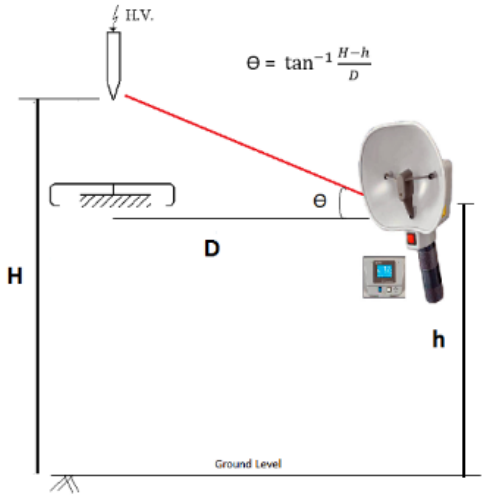


Fig.4.4. Test setup to study the influence of angle of measurement on the measured acoustic sensor.

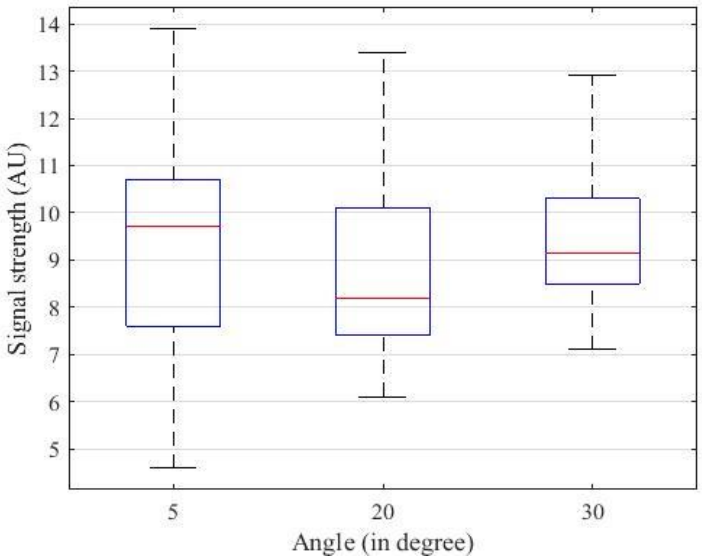


Fig.4.5. Attenuation of the signal strength with the angle of measurement for a 60 Hz component with corona discharge.

## 4.4 Visual representation of frequency component patterns using 3D plots

The low frequency selected features i.e., 60 Hz, 120 Hz, and 180 Hz components, were plotted against one another. The 3-D plots are presented in Figs. 4.6 - 4.8 for controlled PD sources, single disc insulators, and string insulators, respectively.

These plots clearly indicate that the different classes are nonlinearly separable, which means that a nonlinear classifier is required to distinguish among them. As well, the 3-D plots for both single and string insulators also exhibit some similarity with respect to class distribution. It should be noted that the defective sample in the string insulators was always connected to the high voltage end.

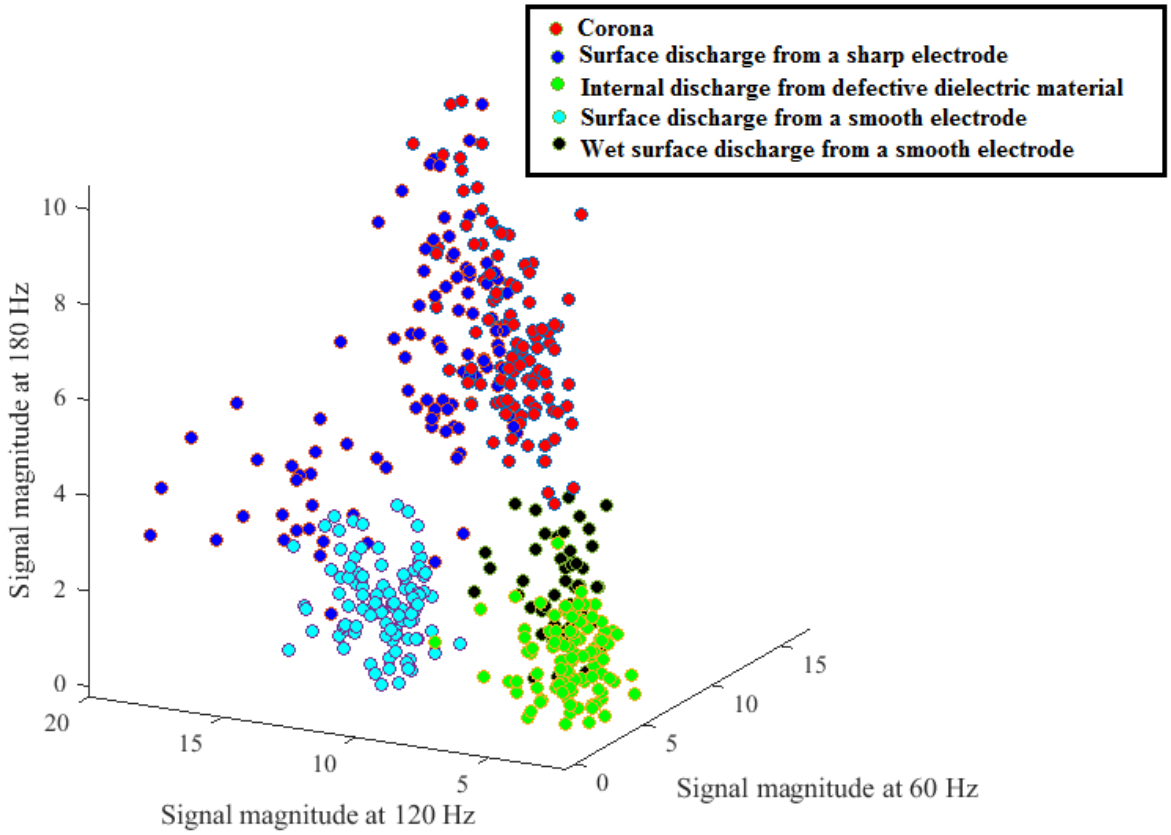


Fig. 4.6. Signal magnitudes for 60 Hz, 120 Hz, and 180 Hz frequency components in controlled PD sources.

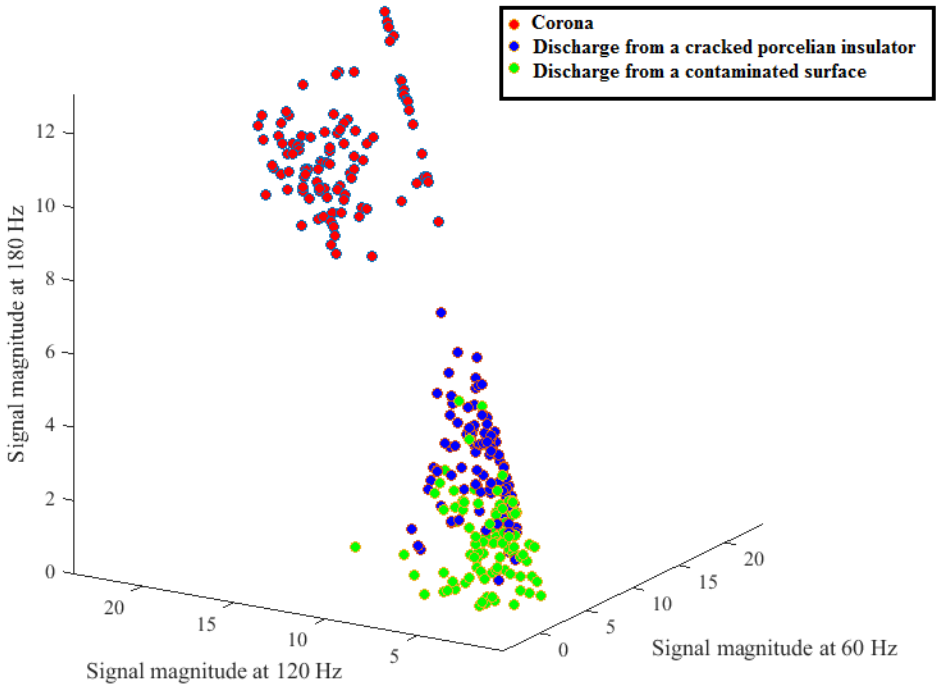


Fig.4.7. Signal magnitudes for 60 Hz, 120 Hz, and 180 Hz frequency components with single insulators.

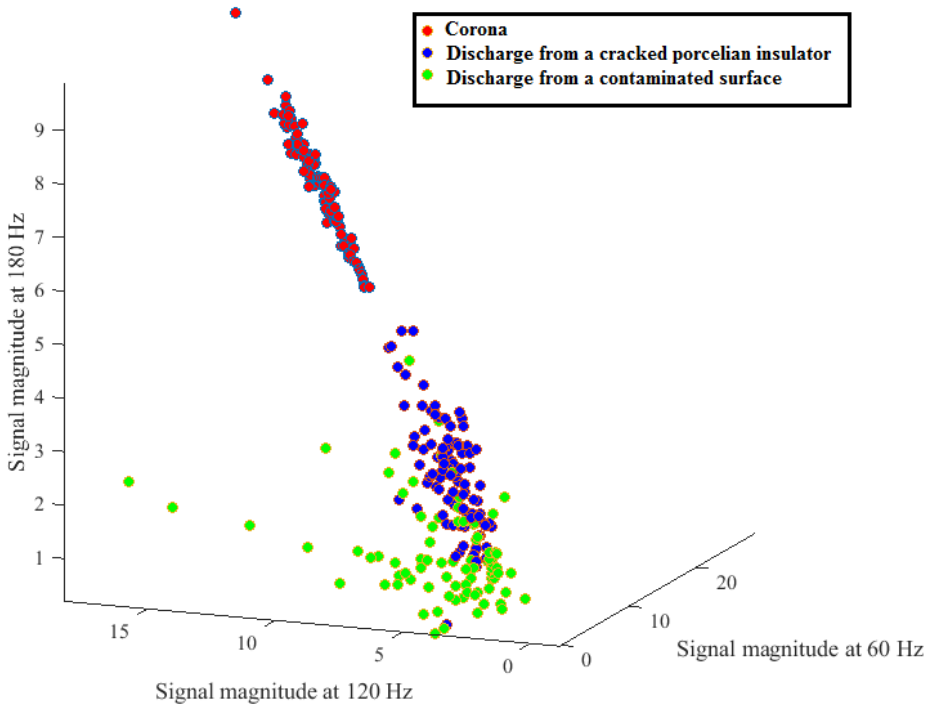


Fig.4.8. Signal magnitudes for 60 Hz, 120 Hz, and 180 Hz frequency components in string insulators.

Moving the position of the cracked insulator to the middle of the three-disc string insulator resulted in a different pattern, as indicated in Fig. 4.9.

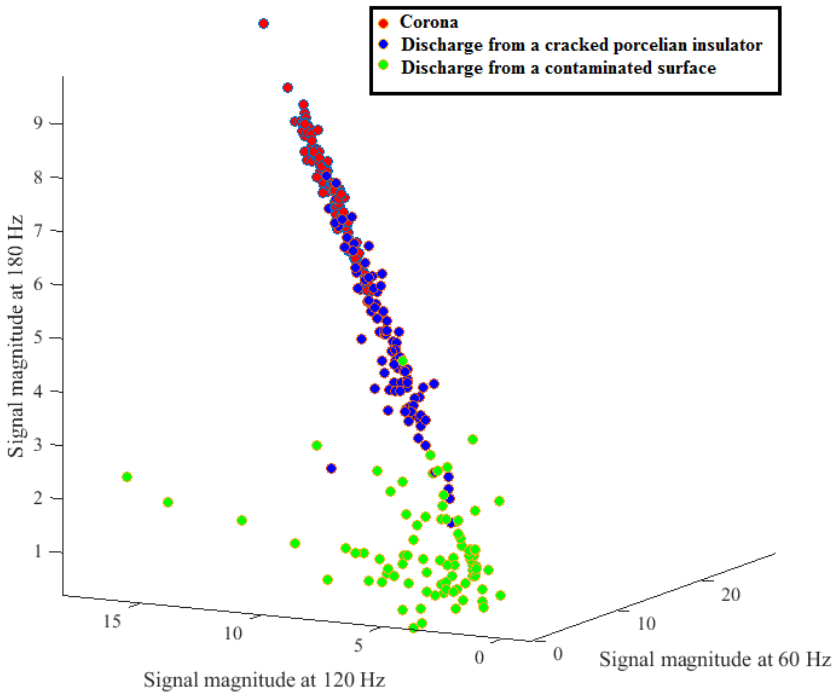


Fig.4.9. Signal magnitudes for 60 Hz, 120 Hz, and 180 Hz frequency components in string insulators with a cracked insulator placed in the middle of the string.

A shift toward the corona cluster and away from the wet discharge can be seen in the cluster representing the discharge from a cracked insulator placed in the middle of the string. This observable shift in the pattern is attributable to the fact that the voltage levels across each disc insulator in the string are not identical, but vary according to the position of the disc. The maximum voltage occurs across the disc nearest to the conductor, while the lowest levels are associated with the disc nearest to the cross arms (grounded conductor). It is also evident that the readings for both the corona and crack insulator classes are mixed together which makes it extremely hard for any classifier to distinguish between them.

## 4.5 Recognition rates for five controlled PD sources

As mentioned in Chapter 3, an ANN classifier was used for the classification of the five different PD types. Total of 450 test data have been collected from five different PD sources. The data was randomly mixed and 70 % of the total data collected is used for training, 15 % for validation, and 15 % for testing. This random mixing of data was repeated for 5 times and the recognition rates are shown in table 4.1. A sample confusion matrix is

shown in Fig. 4.10 and summarizes the classifier recognition rates for the five controlled PD sources. Rows of confusion matrix represent the instances in a predicted class and column represents the instances in an actual class [49].

**Table 4.1: Recognition Rates for the Standalone ANN Classifier Data for Five Controlled PD Sources**

| Trail No. | Class-I | Class-II | Class-III | Class-IV | Class-V | Total recognition rate |
|---|---|---|---|---|---|---|
| 1 | 100 | 100 | 92.3 | 92.9 | 82.4 | 92.6 |
| 2 | 85.7 | 95.2 | 100 | 92.3 | 80 | 91.2 |
| 3 | 83.3 | 100 | 94.1 | 73.3 | 94.1 | 89.7 |
| 4 | 87.5 | 100 | 100 | 93.8 | 93.8 | 95.6 |
| 5 | 77.8 | 94.7 | 100 | 100 | 82.4 | 91.2 |
| Average | 86.86 | 97.98 | 97.28 | 90.46 | 86.54 | 92.06 |

Class-I – wet surface discharge from a smooth electrode; Class-II – surface discharge from a smooth electrode; Class-III – internal discharge from defective dielectric material; Class-IV – surface discharge from a sharp electrode; Class-V – corona.

In the matrix shown in Fig. 4.10, a trend of confusion can be observed between the wet surface discharge from a smooth electrode and the surface discharge from a sharp electrode, and also between the corona and surface discharges from a sharp electrode. Of all the signals, surface discharge from a smooth electrode and internal discharge from a defective insulator stand out as unique and easily distinguishable.

Based on the results, the minimum accuracy level with respect to recognition of different PD groups was 89.7 %, the maximum level was 95.6 %, and average recognition rate was 92 %. The high classification rate shows that the proposed approach in this thesis is clearly able to distinguish the PD associated with variety of PD sources.

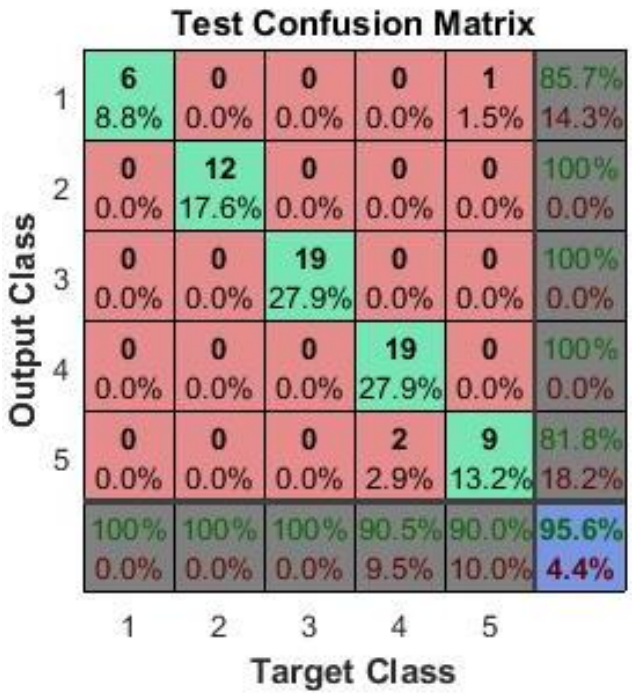


Fig. 4.10. Typical confusion matrix showing individual class recognition rates and total classifier efficiency with respect to distinguishing the PD patterns of five controlled PD sources: Class-I – wet surface discharge from a smooth electrode; Class-II – surface discharge from a smooth electrode; Class-III – internal discharge from defective dielectric material; Class-IV – surface discharge from a sharp electrode; Class-V – corona.

## 4.6 Effect of measurement distance on the classification rates for controlled PD sources based on training and testing with different datasets

An additional case study was conducted in order to observe the behaviour of two classifiers, one of which was trained only with data collected from close proximity (ANN 1) and the other trained with all of the datasets collected from a variety of distances integrated together (ANN 2). Both classifiers were employed for recognizing PD data collected at different distances. Table 4.2 summarizes the recognition rates obtained from the two classifiers.

Although the ANN classifier trained with all of the datasets collected from different distances integrated together produced better recognition results than the other classifier trained with only close-proximity data points, a moderate recognition rate can still be achieved using ANN 1 up to a distance of 250 cm.

**Table 4.2: Comparison of Recognition Rates from Two ANNs: Effect of Distance on Signal Recognition**

| Test data | ANN 1 | ANN 2 |
|---|---|---|
| Training information | Trained only with data collected at 150 cm from the source | Trained with the total data collected at 150 cm, 200 cm, 250 cm, and 300 cm from the source |
| Data collected at 200 cm | 90 % | 98 % |
| Data collected at 250 cm | 82.7 % | 92.2 % |
| Data collected at 300 cm | 70.2 % | 87.8 % |

## 4.7 Effect of the measurement angle on the classification rates for five controlled PD sources

A similar study was conducted in order to investigate the effect of the measurement angle on the recognition rate. One of the ANN classifiers was trained using data measured at a 0° deviation from the line of sight and was then tested using data recorded at 5°, 20°, and 30° deviations. The results are presented in Table 4.3.

The recognition rates for the data measured with different angles of deviation from the PD source were very close. This similar recognition rate between the different angles can be attributed to the similar pattern distribution between the different classes as depicted in Fig. 4.11 for two different angles, i.e., 0 and 30 degree.

**Table 4.3: ANN Recognition Rates: Effect of the Measurement Angle on Signal Recognition**

| Training Data | Recognition Rate |
|---|---|
| Test with 5° of deviation from the source | 84.6 % |
| Test with 20° of deviation from the source | 83.8 % |
| Test with 30° of deviation from the source | 85.8 % |

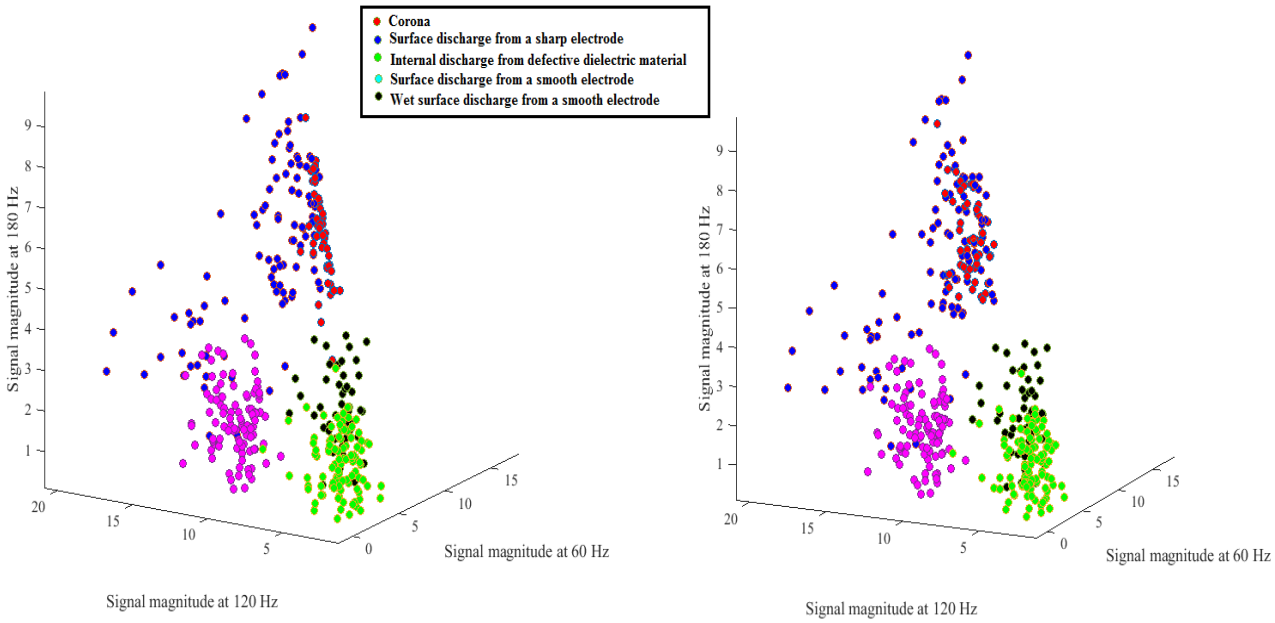


(a) (b)

Fig. 4.11. Pattern formations for (a) a 0° deviation and (b) a 30° deviation.

## 4.8 Application of the classifier for porcelain insulator condition monitoring

Total of 300 test data have been collected from single-disc and string insulator arrangements. The data was randomly mixed and 70 % of the total data collected is used for training, 15 % for validation, and 15 % for testing. Tables 4.4 and 4.5 show the recognition rate obtained from five sets of testing sessions conducted using the two classifiers.

The average recognition rates with single-disc and string insulators were 89.34 % and 87.54 %, respectively. The good recognition rates show the huge potential for the application of the acoustic emission (AE) technique with respect to detecting defects and surface conditions in porcelain line insulators, and as a tool for condition monitoring applications.

**Table 4.4: Classifier Recognition Rates for Acoustic Data Recorded from a Single-Disc Line Insula**tor

| Trail No. | Class-I | Class-II | Class-III |
|---|---|---|---|
| 1 | 100 % | 80 % | 82.4 % |
| 2 | 100 % | 92.3 % | 76.5 % |
| 3 | 100 % | 100 % | 88.9 % |
| 4 | 100 % | 80 % | 85.7 % |
| 5 | 100 % | 78.6 % | 81.8 % |
| AVG | 100 % | 86.18 % | 83.06 % |

Class-I: corona; Class-II: discharge from a cracked line insulator; Class-III: discharge from a contaminated surface.

**Table 4.5: Classifier Recognition Rates for Acoustic Data Recorded from a String Insulator Arrangement.**

| Trail No. | Class-I | Class-II | Class-III |
|---|---|---|---|
| 1 | 100 % | 81.3 % | 87.5 % |
| 2 | 100 % | 100 % | 66.7 % |
| 3 | 100 % | 91.7 % | 84.2 % |
| 4 | 100 % | 93.8 % | 86.7 % |
| 5 | 100 % | 50 % | 75 % |
| AVG | 100 % | 83.36 % | 80.02 % |

Class-I: corona; Class-II: discharge from a cracked line insulator; Class-III: discharge from a contaminated surface.

Based on the similarity of the single-disc and string insulator pattern formations, a single ANN classifier was trained using the data obtained from the three single porcelain disc samples and then tested on the string insulator datasets. Table 4.6 shows the five sets of test results, and Fig. 4.11 presents a sample confusion matrix of the test results.

The average recognition rate for discharge produced from corona, wet surface discharge and cracked insulator were 98.04 %, 66.4 %, and 62.84 % respectively. It is apparent from these results that each insulator arrangement (single disc vs three discs) need to be trained and tested separately.

**Table 4.6: Recognition Rates Obtained from a Classifier Trained Using Single-Disc Insulator Data and Tested on String Insulator Data**

| Trail No | Class-I | Class-II | Class-III | Total Recognition Rate |
|---|---|---|---|---|
| 1 | 97.7 % | 64.6 % | 63.2 % | 73.7 % |
| 2 | 97.6 % | 68.2 % | 69 % | 76.7 % |
| 3 | 97.6 % | 65.5 % | 66.9 % | 75 % |
| 4 | 100 % | 55.3 % | 65.2 % | 70 % |
| 5 | 97.3 % | 60.6 % | 67.7 % | 72.7 % |
| AVG | 98.04 % | 62.84 % | 66.4 % | 73.62 % |

Class-I: corona; Class-II: discharge from a cracked line insulator; Class III: discharge from a contaminated surface

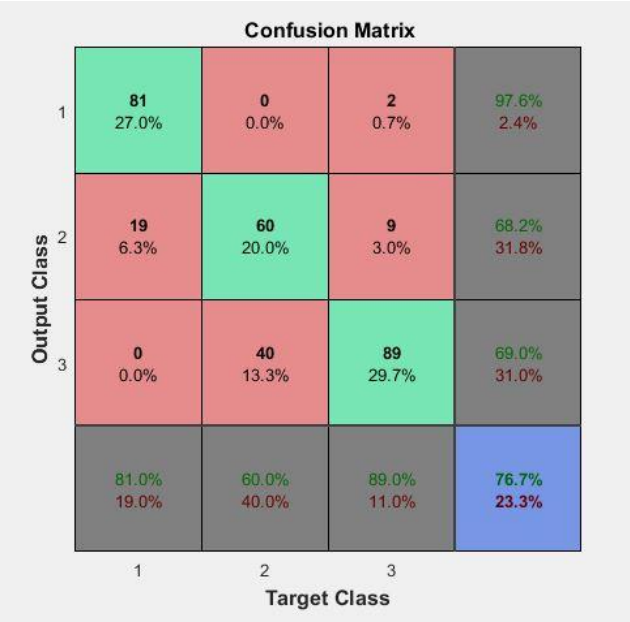


Fig. 4.12. Typical confusion matrix showing individual class recognition rates and total classifier efficiency with respect to distinguishing PD patterns from a classifier trained with data recorded from a single-disc insulator and tested with data recorded from a string insulator: Class I – corona; Class II – discharge from a cracked line insulator; Class III – discharge from a contaminated surface.

# 4.9 Analysis with varied insulator disc positions

To study the robustness of the proposed technique, investigations included an examination of the effect on the recognition rate when the insulator disc position was varied. Table 4.7 presents the five sets of test results obtained from the ANN classifier.

**Table 4.7: Recognition Rates Obtained from an ANN Classifier Trained with Data Collected from a Three-Disc Insulator String with a Cracked Middle Disc**

| Trail No. | Class-I | Class-II | Class-III | Total Recognition Rate |
|---|---|---|---|---|
| 1 | 75 | 92.9 | 90.9 | 84.4 |
| 2 | 86.4 | 73.3 | 100 | 84.4 |
| 3 | 83.3 | 90.9 | 100 | 91.1 |
| 4 | 78.6 | 76.5 | 92.9 | 82.2 |
| 5 | 80 | 84.6 | 100 | 88.9 |
| AVG | 80.66 | 83.64 | 96.58 | 86.2 |

Class-I: corona; Class-II: discharge from a cracked line insulator; Class-III: discharge from a contaminated surface

The average recognition rate was 86.2 %, which was very close to that for a defective insulator placed near the high voltage supply end. It can be observed that the recognition rate for class-I (i.e., corona, was compromised, and that the recognition rate for the class-III wet surface discharge was elevated. Based on this analysis, it is clear that the classifier is able to differentiate defects based on the type of defect, and that the position of the defects has a low impact on the overall recognition rate.

# Chapter 5

# Conclusion and Suggestions for Future Work

## 5.1 Summary and conclusion

The primary goal of this research was to investigate a feasibility index for detecting and classifying different types of electrical discharge using acoustic emission (AE) signatures. An additional objective was to explore ways of applying the knowledge gained in classifying different types of discharge so that it could be used for the condition monitoring of ceramic line insulators. To this end, numerous experiments were conducted in order to assess a variety of controlled PD signatures and defective line insulators, both in string and single-disc conditions. Based on the results, the following conclusions can be drawn:

1) Each type of controlled PD source produced a unique acoustic signature, which were analyzed further using signal-processing tools.

2) Distinguishable patterns were observed using acoustic signal magnitudes of 60 Hz, 120 Hz and 180 Hz, with the results further enhanced by employing the ANN for differentiating PD sources with signal magnitude data at 60 Hz, 120 Hz, and 180 Hz as input features.

3) The trained classifier has been proven effective for the classification of each specific type of controlled PD, with a high degree of accuracy: more than 90 %.

4) Through repetitive measurements, the impact of angular and linear distance variations on the measurement of acoustic signals was examined. The findings revealed that the amplitude of the measured acoustic signal decreased with increases in the linear and angular distances from the sample. Angular deviation was more sensitive to distance with respect to acoustic sensor measurements.

5) The study was extended to include the classification of defects and contamination conditions in both string and individual insulators. In this regard, the classifier produced a recognition rate of more than 85 %.

6) Varying the position of a cracked insulator disc within a string has only a very small effect on the level of classification performance.

## 5.2 Future work

A number of challenges can be addressed based on the work presented in this thesis. Important possibilities for future work are highlighted in the following sections.

### 5.2.1 Applications in the field

All of the experiments described in the thesis were conducted in a noise-free and completely shielded environment. The laboratory was free from any of the external interference that is generally present in a field environment. A set of selective noise levels shall be generated in laboratory and their effect on acoustic signal measurement to be studied in the first place and later environmental factors on the strength of the acoustic signals to be studied in the field.

### 5.2.2 Increasing the number of line insulators in the string

The study performed in this research was limited to the use a string of insulators consisting of three porcelain disc insulators. Future work should consider studying the effect of increasing the number of discs in the string and also changing the defect location in the string.

### 5.2.3. Relationship between acoustic signal and conventional measurement techniques

In conventional PD measurement techniques, the apparent charge is generally quantified by a band-pass filter, as specified in IEC 60270. Unlike apparent charge measurements, acoustic measurement techniques are not subject to any well-established standards. For acoustic measurement techniques to become well accepted, correlations should be established between acoustic signal measurements and actual PD signatures identified according to IEC 60270.

### 5.2.4. Extending testing to include defective polymeric and other ceramic models

With ceramic insulators, utilities encounter major problems created by punctured insulators, which can also become a safety hazard for the linemen who generally perform contact-based testing and maintenance work. Although the current work was limited to cracking, contamination, and hardware defects, future work could include collaboration with industry in order to collect punctured samples, and the AI classifier library could be updated to incorporate the data collected from the testing of punctured samples of both individual and string insulators. The work presented in the thesis should also be extended to incorporate different types of defective polymeric insulators, which are widely used as replacements for ceramic insulators.

### 5.2.5. Unmanned aircraft-mounted PD measurement and classification systems

The ultimate aim of this work is to create an online AI-powered device that can differentiate PD from practical insulation systems. The developed prototype could be mounted on top of a drone that could fly close to line insulators, collect the required data samples, and determine the type of defect. In this way, this method would ensure complete human safety and could also contribute to future smart systems.

# List of publications in refereed conference proceedings

1. Satish Kumar Polisetty, Shesha Jayaram and Ayman El-Hag “Partial Discharge Classification Using Acoustic Signals and Artificial Neural Networks” ,Electrostatics Joint Conference, Boston University, Boston, USA, June 17-20, 2018.

# References


[1] E.Kuffel, W.S.Zaengl, and J.Kuffel, *High Voltage Engineering-Fundamentals*. Butterworth-Heinemann, 2000.

[2] (https://suwalls.com/photography/transmission-tower-31754/)(Accessed: 2018-08-21).

[3] R.S.Gorur, E.A. Cherney, and J.T. Burnham, outdoor Insulators. Ravi S. Gorur, Inc., 1999.

[4] J.S.T.Loom, "Insulators for High Voltage". Peter Peregrinus Ltd., London, 1988.

[5] E.A.Cherney, "Non-ceramic insulators-a simple design that requires careful analysis," IEEE Electrical Insulation Magazine, vol.12, no.6, pp.7-15, 1996.

[6] E.A.Cherney, "RTV Silicon-a high tech solution for a dirty insulation problem," IEEE Electrical Insulation Magazine, Vol.6, no.3, pp.8-14, 1995.

[7] R.S. Gorur, D.Shaffner, W.Clark and R.Vinson, "Utilities Share Their Insulator Field Experience," Transmission and Distribution World, 57(4), 17-27, 2005.

[8] "IEEE Guide for Maintenance Methods on Energized Power Lines," in IEEE Std 516-2009, pp.1-144, 24 June 2009.

[9] Mishra, A.P., Gorur R.S., & Venkataraman, S. (2008). Evaluation of porcelain and toughened glass suspension insulators removed from service. Dielectrics and Electrical Insulation, IEEE Transaction on, 15(2), 467-475.

[10] S-H.Kim, E.A.Cherney, R.Hackam, and K.G.Rutherford, "Chemical changes at the surface of RTV silicone rubber coatings on insulators during dry-band arcing," IEEE Transaction on Dielectric and Electrical Insulation, Vol.1, no.1, pp.106-123, 1994.

[11] (https://people.en.made-in-china.com/product/DykELghuJrcR/China-High-Quality-PinPolymeric-Insulator-for-High-Voltage-Overhead-Transmission-Line.html.)(Accessed: 2018-08-24).

[12] (https://www.ofilsystems.com/news/history.html.)(Accessed: 2018-08-23).

[13] (https://electrical-engineering-portal.com/ceramic-porcelain-and-glass-insulators.)(Accessed: 2018-09.01).

[14] E.Cherney and R.Hooton,"Cement growth failure mechanism in porcelain suspension insulators," IEEE Transaction on Power Delivery, vol.2, no.1, pp.249-255, 1987.

[15] (http://www.inmr.com/reviewing-modes-of-insulator-failure/)(Accessed: 2018-09-10).

[16] (http://advanceengineers.blogspot.com/2010/07/overhead-line-insulators.html.)(Accessed: 2018-09-11).

[17] L. Grigsby, "The electric power engineering handbook," CRC Pr I Llc, 2001. 13.

[18] K. Naito, Y. Mizuno, and W. Naganawa, "A study on probabilistic assessment of contamination flashover of high voltage insulator," Power Delivery, IEEE Transactions on, vol. 10, no. 3, pp. 1378–1384, Jul 1995. 13.

[19] R.Brown and B.Humphrey, "Asset management for transmission and distribution," Power and Energy Magazine, IEEE, vol.3, no.3, pp. 39-45, 2005.

[20] A.Naderian et al.,"best practices for transmission line insulator condition assessment," CEATI Int. Inc., Montreal, ON, Rep.T123700-3239, Apr.2014.

[21] R.Gorur, Bob Olsen, Art Kroese, Fred Cook and Senthil Kumar S," Evaluation of critical components of Non-Ceramic Insulators (NCI) In-Service: Role of Defective Interfaces," PSERC Publications, August 2004.

[22] R.Williams and G.Williams," Ultraviolet, Infrared and Fluorescence Photography," medical and scientific photography, 2005.

[23] A.J. Phillips, C.S. Engelbrecht, "the feasibility of using daytime corona inspection to identify contaminated insulators that needs to be washed", CIGRE B2-213, Paris, 2008.

[24] H. Shaffner, "experience with a composite insulator testing instrument based on the electric field method", ESMO 2000, Montreal, Canada, October 2000.

[25](http://www.ee.co.za/wp-content/uploads/2016/07/EngineerIT-July-2016-36-37-2.jpg.) (Accessed: 2018-11-02).

[26] El-Sayed M. El-Refaie, M.K. Abd Elrahman, M. Kh.Mohamed, "Electric field distribution of optimized composite insulator profiles under different pollution conditions" Ain Shams Eng. J. (2016).

[27] IAEA.Guidebook on Non-Destructive Testing of Concrete Structures; IAEA: Vienna, Austria, September 2002.

[28] CIGRE Working Group B2.03, Guide for the assessment of old cap & pin and long rod insulators made of porcelain or glass: What to check and when to replace, Oct. 2006.

[29] S. Anjum, S. Jayaram, A. El-Hag and A. N. Jahromi, "Detection and classification of defects in ceramic insulators using RF antenna," in IEEE Transactions on Dielectrics and Electrical Insulation, vol. 24, no. 1, pp. 183-190, Feb. 2017.

[30] Yaacob, M. M.; Alsaedi, M. A.; Rashed, J. R.; Dakhil, A. M.; Atyah, S. F., " Review on partial discharge detection techniques related to high voltage power equipment using different sensors," Photonic Sensors, Volume 4, Issue 4, pp.325-337.

[31] (http://zfp.cbm.bgu.tum.de/mediawiki/index.php/Ultrasonic_Pulse-Echo_Method.)(Accessed: 2018-09-26).

[32] K. L. Wong, "Application of very-high-frequency (VHP) method to ceramic insulators," in IEEE Transactions on Dielectrics and Electrical Insulation, vol. 11, no. 6, pp. 1057-1064, Dec. 2004.

[33] A. Cavallini, S. Chandrasekar, G. C. Montanari and F. Puletti, "Inferring ceramic insulator pollution by an innovative approach resorting to PD detection," in IEEE Transactions on Dielectrics and Electrical Insulation, vol. 14, no. 1, pp. 23-29, Feb. 2007.

[34] S. Anjum, A. El- Hag, S. Jayaram and A. Naderian, "Classification of defects in ceramic insulators using partial discharge signatures extracted from radio frequency (RF) signals," 2014 IEEE Conference on Electrical Insulation and Dielectric Phenomena (CEIDP), Des Moines, IA, 2014, pp.

[35] Krautkramer H., KrautkramerJ. "Ultrasonic Testing of Materials," Springer, London, U.K., 1990.

[36] D. W. Auckland, C. D. Smith and B. R. Varlow, "Detection of degradation in opaque dielectrics by ultrasound," [1992] Proceedings of the 4th International Conference on Conduction and Breakdown in Solid Dielectrics, Sestri Levante, Italy, 1992, pp. 343-347.

[37] McGrail A.J., Risino A., Auckland D.W., Varlow B.R. "Application of a Medical Ultrasound scanner to the inspection of high voltage insulation," IEEE Electrical Insulation magazine, Vol.9, No.6, November 1993.

[38] Zhu D., McGrail A.J., Auckland D.W., Varlow B.R., Swingler S. "Partial Discharge Detection in Cable Termination using Acoustic Emission Techniques and Adaptive Signal Processing," IEEE International Symposium on Electrical Insulation, Pittsburgh, USA, June 1994.

[39] (http://www.hydroquebec.com/innovation/en/pdf/2010G080-21A-DIF.pdf)(Accessed: 2018-10-16).

[40] C.M.Pei, N.Q.Shu, L.Li, Z.P.Li and H.Peng "On-line monitoring of insulator contamination-causing flashover based on acoustic emission," DRPT2008 6-9 April 2008 Nanjing China.

[41] C Nyamupangedengu, L P Luhlanga and T Lettape "Acoustic and HF detection of defects on porcelain pin insulators,'" 2007 IEEE Power Engineering Society Conference and Exposition in Africa-PowerAfrica, Johannesburg, 2007, pp.1-5.

[42] A. El-Hag, S. Mukhopadhyay, K. Al-Ali and A. Al-Saleh, "An intelligent system for acoustic inspection of outdoor insulators," 2017 3rd International Conference on Condition Assessment Techniques in Electrical Systems (CATCON), Rupnagar, 2017, pp. 122-125.

[43] F.H. Kreuger, Discharge Detection in High Voltage Equipment, Butterworth-Heinemann, 1989.

[44] R. T. Harrold, "Acoustic Waveguides for Sensing and Locating Electrical Discharges in High Voltage Power Transformers and Other Apparatus," in IEEE Transactions on Power Apparatus and Systems, vol. PAS-98, no. 2, pp. 449-457, March 1979.

[45] EPRI EL – 4009 Project 426 – 1 report: "Acoustic Emission Detection of Partial Discharges in Power Transformers".

[46] R. Bozzo, F. Guastavino. Department of Electrical Engineering, University of Geneva, G. Guerra, ABB Corporate Research, Milano, Italy. "PD Detection and Localization by means of Acoustic Measurements on Hydro generator Stator Bars" 1995 IEEE.

[47] (https://www.linkedin.com/pulse/guide-understanding-partial-discharge-sensor-dustin-ashliegh.)(Accessed: 2018-08-11).

[48] MK-720 product data sheet, Available: https://www.abqindustrial.net/store/industrial-maintenance-c102/corona-discharge-detector-c-102_72/mk720-corona-discharge-detector-p-993.html.

[49] (https://en.wikipedia.org/wiki/Confusion_matrix./)(Accessed: 2018-11-21).